

**Fundamental studies of non-premixed
combustion in turbulent wall jets using direct
numerical simulation**

by

Zeinab Pouransari

September 2011
Technical Reports from
Royal Institute of Technology
Department of Mechanics
SE-100 44 Stockholm, Sweden

Akademisk avhandling som med tillstånd av Kungliga Tekniska Högskolan i Stockholm framlägges till offentlig granskning för avläggande av teknologie licentiatexamen onsdagen den 28 september 2011 kl 10.15 i V2, Kungliga Tekniska Högskolan, Teknikringen 76, Stockholm.

©Zeinab Pouransari 2011

Universitetsservice US-AB, Stockholm 2011

Fundamental studies of non-premixed combustion in turbulent wall jets using direct numerical simulation

Zeinab Pouransari

Linné FLOW Centre, KTH Mechanics, SE-100 44 Stockholm, Sweden

Abstract

The present thesis deals with the fundamental aspects of turbulent mixing and non-premixed combustion in wall-jet flows. Direct numerical simulations (DNS) of compressible turbulent flows are performed in a wall-jet configuration, which has a close resemblance to many industrial combustion applications. The triple "turbulence-chemistry-wall" interactions are also present in this flow set-up. These interactions have been addressed by first focusing on turbulent flow effects on the isothermal reaction, including the near-wall issues. Then, by adding heat-release to the simulations, it has been concentrated on heat-release effects on various phenomena that occur in the reacting turbulent wall-jet flow. In the computational domain, fuel and oxidizer enter separately in a non-premixed manner and the flow is fully turbulent and subsonic in all simulations. In the first phase of this study, the case of a turbulent wall-jet including an isothermal reaction without heat release is addressed in order to isolate the near-wall effects and the mixing characteristics of the flow and the key statistics for combustion are studied in the absence of thermal effects. A deeper insight into three-dimensional mixing and reaction characteristics in a turbulent wall-jet has been gained through investigation of the probability density functions, higher order moments of velocities and reacting scalars and the scalar dissipation rates of different species. In the second phase, DNS of turbulent reacting wall-jets including heat release is performed, where a single-step global exothermic reaction with an Arrhenius-type reaction rate is considered. The main target was to identify the heat-release effects on different mixing scales of turbulent wall-jet flow. The scalar dissipation rates, time scale ratios, two-point correlations, one and two-dimensional premultiplied spectra are used to illustrate the heat release induced modifications. It is observed that heat release effects delay the transition process in the chemically reacting cases and enlarge the fluctuation intensities of density and pressure, but have a damping effect on all velocity fluctuation intensities. Finer small mixing scales were observed in the isothermal simulations and larger vortical structures formed after adding significant amounts of heat-release. Simulations with different Damköhler numbers, but comparable temperature-rise are performed and the expected behavior, a thinner flame with increasing Damköhler number, is observed. Finally, some heat transfer related quantities are examined. The wall heat flux and the corresponding Nusselt numbers are addressed. The near-wall reaction effects on the skin friction coefficient are studied and further the reaction characteristics are investigated throughout the domain.

Descriptors: Turbulence, non-premixed combustion, global reaction, direct numerical simulation, wall-jet, heat release, mixing scales, heat transfer

Preface

The present thesis deals with the fundamentals of turbulent mixing and non-premixed combustion in wall-jet configurations. An introduction to turbulent combustion simulations and the turbulent wall-jet set-up is provided in the first part. The second part contains the following three papers.

Paper 1. Z. POURANSARI, G. BRETHOUWER AND A. V. JOHANSSON, 2011
Direct numerical simulation of an isothermal reacting turbulent wall-jet,
Physics of Fluids, **23** 085104

Paper 2. Z. POURANSARI AND A. V. JOHANSSON, 2011
Heat release effects on mixing scales of turbulent reacting wall-jets: a direct numerical simulation study

Paper 3. Z. POURANSARI AND A. V. JOHANSSON, 2011
Numerical investigation of wall heat transfer and skin-friction coefficient in reacting turbulent wall-jets

Division of work between authors

The main advisor of the project is Prof. Arne V. Johansson (AJ) and the co-advisor was Dr. Geert Brethouwer (GB).

Paper 1.

Numerical simulations were performed by Zeinab Pouransari (ZP). Constant discussion was being held between ZP, GB and AJ for interpretation of the results. The paper was written by ZP with feedback from AJ and GB.

Paper 2.

Development of the relevant subroutines was done by ZP. Numerical simulations and interpretation of results were carried out by ZP in collaboration with AJ. Paper was written by ZP with input from AJ.

Paper 3.

Numerical simulations were performed by ZP with continuous input from AJ. Paper is written by ZP and feedback and comments were provided by AJ.

Contents

| | |
|--|-----|
| Abstract | iii |
| Preface | iv |
| Part I | 1 |
| Chapter 1. Introduction | 2 |
| Chapter 2. Governing equations | 7 |
| 2.1. Conservation equations | 7 |
| 2.2. Chemical reaction | 10 |
| 2.3. Important non-dimensional numbers | 11 |
| 2.4. Averaging principles | 14 |
| Chapter 3. Simulations of non-premixed combustion | 15 |
| 3.1. Combustion simulation overview | 15 |
| 3.2. Combustion modeling | 18 |
| 3.3. Premixed and non-premixed combustion modeling | 18 |
| 3.4. Non-premixed combustion modeling tools | 19 |
| Chapter 4. Turbulent wall-jet | 24 |
| 4.1. Wall-jet set-up and background | 24 |
| 4.2. Scalings for compressible turbulent wall-jet | 27 |
| 4.3. DNS of reacting turbulent wall-jets | 28 |
| Chapter 5. Summary of the papers | 38 |
| Outlook | 40 |
| Acknowledgments | 41 |
| Bibliography | 42 |

Part I

Introduction

CHAPTER 1

Introduction

The industrial power available to mankind is still mainly provided by the chemical energy stored in hydrocarbon fossil fuels. The combustion process, through which the fuel is burned and the chemical energy is released, is of crucial importance to almost every engineering process. Combustion is an applied science that is important in transportation, power generation, industrial processes, chemical engineering and aeronautical applications.

Today, the number of combustion systems used in transportation and transformation industries is rapidly growing. People want to travel faster and at the same time pollution and environmental problems are becoming critical issues in our societies. The negative environmental impacts of excessive fossil fuel combustion are becoming evident. Emissions of CO_2 contribute to global warming. Other pollutants such as unburnt hydrocarbons, soot and nitrogen oxides also have a negative impact on the environment. More rigorous regulations concerning emissions are presently enforced in the automotive industry and on power plants to reduce emissions and their environmental impact. Thus, we need to be able to improve our combustion technology accordingly. To reach these goals, an improved understanding of combustion and mixing processes is needed, as well as improved models to be used in the development of cleaner combustion applications.

The combustion mechanism needs to be understood together with turbulence for two reasons. Turbulence often increases the mixing process and enhances combustion, on the other hand, combustion releases heat which generates gas expansion and density variation that influences the turbulent flow. While the mixing process in turbulent flows is known to be associated to the local strain rate, but the details of the mixing process in turbulent flows remain to be explained more quantitatively. Besides, the structure of the turbulent flow is not yet fully understood and the mixing prediction remains to be a challenge. The unresolved problems in turbulence seem to become even more complicated in turbulent combustion systems. The interaction of turbulent mixing with chemical reaction is even less explored. Moreover, this interaction can get substantially affected by the presence of walls, which is the case in most combustion systems. Some of these interactions are outlined in figure (1.1). In practice, combustion must simultaneously be safe, efficient and clean. Thus, different interactions involved in the turbulent reacting flows need to be understood, in order to enhance different aspects of the performance of

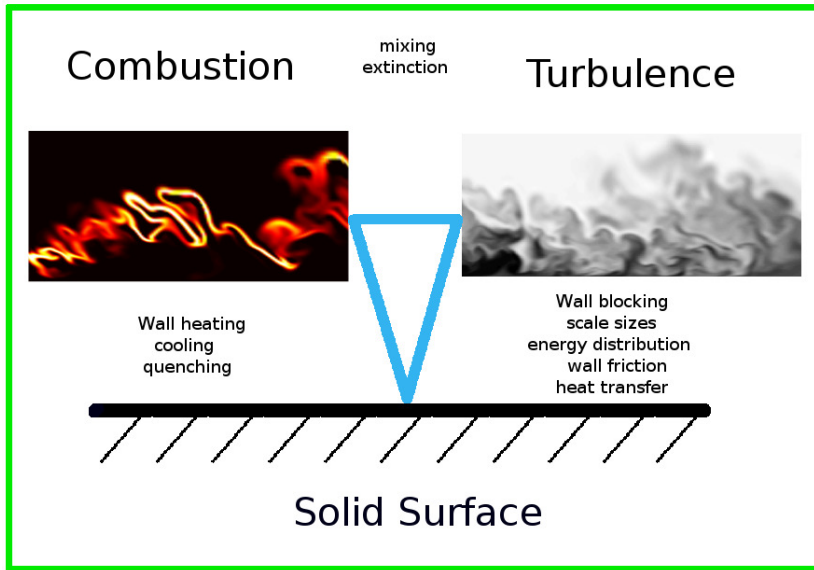


FIGURE 1.1. The triple interaction between the wall, turbulence and combustion.

the combustion systems. To burn as efficient as possible, we need to mix better and at the same time take care of the flame stability, all these are not possible without obtaining accurate information about the turbulent flow field.

Studying the mechanisms involved in turbulent combustion flows has been the objective of numerous theoretical, experimental and numerical works in the last century. Combustion can be classified according to several criteria and one of the most common classifications is made depending on the way the reactant species are mixed prior to entering the combustion chamber. Consequently, the academic universe of combustion science is divided into two regimes, namely non-premixed and premixed combustion, where in the former, fuel and oxidizer are separated prior to burning and in the latter, they are mixed before ignition. However, one needs to be aware of the fact that this division is more of an academic importance and a definite border does not exist in practical situations whereas many fuels burn in partially premixed conditions. The present work deals with a non-premixed case, which is also more widely used in industrial applications, due to safety reasons.

Turbulent reacting flows in general and combustion systems in particular have been tackled both numerically and experimentally. The experimental works have advanced our understanding of the turbulent combustion systems enormously in the past decades. Although, the recent simultaneous measurements of turbulent velocity fields and the reacting scalar concentrations together with local temperature, has helped us to gain a more realistic picture of

the burning process, however, obtaining detailed information from high quality computations seems to be necessary for gaining insight into the fundamentals of the physics of the turbulence-chemistry interaction. An important practice is to implement our state-of-the-art knowledge, gained from well designed numerical simulations, into our combustion models. Modeling of turbulent combustion is a challenging task. In turbulent flames, various difficulties such as strong heat-release, complex chemistry and large ranges of time and length scales are added to the conventional complexities present in constant-density turbulent flows. Thus, both turbulence and combustion models need to be improved and this needs to be done in a meaningful way. The new models are expected to predict much wider ranges of turbulent combustion regimes and, of course, to be more accurate.

Setting up this goal in mind, to shed light into the fine grained interactions tangled in the turbulent reacting flows and even more, in the near-wall regions, perhaps only direct numerical simulation can be an appropriate candidate for high fidelity computations. In direct numerical simulation, all different scales of the flow as well as the flame structure are meant to be resolved. The exact definition of direct numerical simulation in reacting flows, is a subject of further discussion, which will briefly be addressed in chapter 3.

Many combustion applications in confined domains contain regions where mixing and reaction take place close to a wall, thus better understanding of the wall effects plays an essential role in gaining insight into the full problem. The turbulent plane wall-jet flow has close resemblance to a wide range of mixing and combustion applications. In particular, the interactions of reaction and mixing with walls are of great interest in the wall-jet configuration. A schematic of a turbulent plane wall-jet flow can be seen in figure (1.2) which shows the instantaneous snapshots of temperature and streamwise velocity fields. The structure of a developed turbulent wall-jet can formally be described as two adjacent shear layers of different character. The small scales of turbulence are present close to the wall whereas larger scales exist in the outer shear region, and this makes the turbulent wall-jet a valuable test case for reaction and mixing applications.

In the present study the main objective is to examine the triple interaction between turbulent mixing, chemical reaction and the wall effects. The primary target is to investigate the mixing characteristics together with the near-wall behavior of the reacting species as well as the reaction rate in the turbulent reacting wall-jet configuration. The present study is not intended to present a realistic chemical reaction, but it is rather an exploratory study to demonstrate the fundamental mixing and reaction characteristics by analyzing the key statistics for combustion, such as the probability density functions, higher order moments of the scalar concentrations, turbulent kinetic energy and the scalar dissipation rates.

In order to do so, the investigation is started by performing direct numerical simulations of an isothermal reacting turbulent wall-jet flow. In the first part

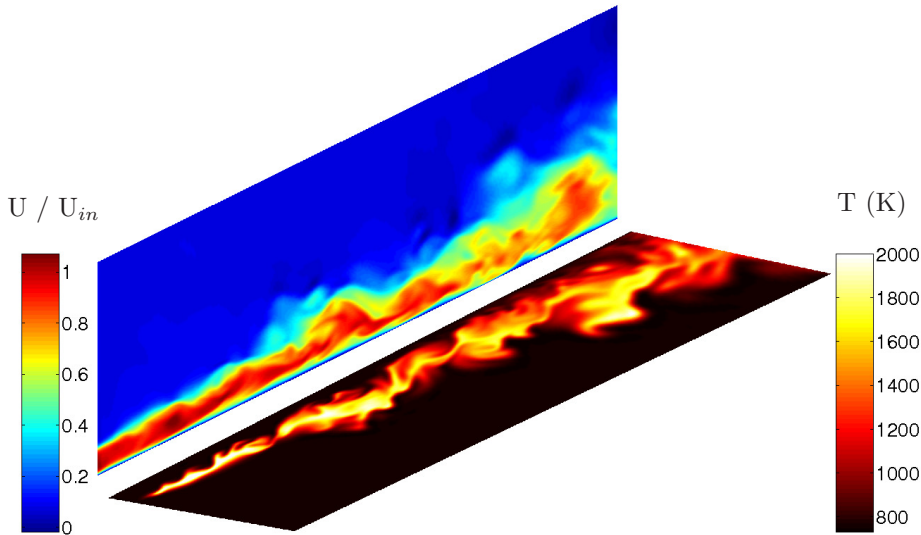


FIGURE 1.2. Snapshots of the instantaneous streamwise velocity (upper) and temperature (lower) fields for a reacting turbulent plane wall-jet flow; The flow is from left to right.

of this study, the flow is uncoupled from the reaction, the influence of turbulent mixing on the reactions is studied in the absence of temperature effects. This part of our study disregards the effects of chemical reactions on the turbulent flow field intentionally and thus it can concentrate on the turbulent flow effects on the isothermal reaction. The focus is on mixing properties which gives valuable material for comparison to the following study, where heat-release is added.

In the second phase of this study, exothermic reactions are considered and direct numerical simulation of turbulent reacting wall-jets including significant amounts of heat-release are performed. The heat-release effects are indeed very important in reacting flows in general and also in the present turbulent wall-jet set-up. Moreover, the flame-wall interactions are of crucial importance, both in the isothermal reaction framework and even more in the presence of heat-release effects, as was mentioned earlier. Thus, in this part, we have concentrated more on heat-release effects on the turbulent flow field and the turbulence-chemistry interactions present in the turbulent wall-jet configuration, including the near-wall behavior.

The rest of this exposition is organized as follows. Chapter 2 exhibits the governing equations for both the flow field as well as the basic equations for the chemical reaction. In chapter 3, the turbulent combustion simulation is addressed in general sense with emphasis on direct numerical simulation of non-premixed turbulent reacting flows and in particular those studies involving

flame-wall interaction. In this chapter, some basics of combustion modeling tools are included. This part is intentionally being kept brief and only those issues which are of relevant importance for the DNS data analysis are accentuated. Turbulent wall-jet flow is introduced in chapter 4, where different types of wall-jet configurations are described. Besides, different scalings, which are used for presenting the results are introduced and discussed. Some parts of the results, both from the isothermal reaction case and the heat-release effect investigation are included in this chapter. A summary of the papers, presented in part II of this thesis, may be found in chapter 5, which consists the main conclusions of this study and is followed by the outlook for future research.

CHAPTER 2

Governing equations

In direct numerical simulation (DNS) of turbulent reacting flows the governing equations of compressible flow and the transport equations of the participating species must be solved. Below, the governing equations of a compressible reacting multicomponent fluid, containing n species, are presented. The notation follows Poinso & Veynante (2001) and the derivations of the equations, based on the conservation of mass, momentum and energy, can be found in reference works such as Williams (1985) and Turns (1993).

2.1. Conservation equations

2.1.1. Conservation of mass and momentum

The global mass conservation equation for compressible flows is expressed as

$$\frac{\partial \rho}{\partial t} + \frac{\partial \rho u_i}{\partial x_i} = 0, \quad (2.1)$$

where ρ is the mass density and u_i is the velocity vector.

The momentum conservation equation, valid for both reacting and non-reacting flows reads

$$\frac{\partial \rho u_i}{\partial t} + \frac{\partial \rho u_i u_j}{\partial x_j} = -\frac{\partial p}{\partial x_i} + \frac{\partial \tau_{ij}}{\partial x_j} + F_i. \quad (2.2)$$

Here τ_{ij} represents the viscous stress tensor and F_i represents a body force. For a Newtonian fluid the viscous stress tensor is defined as

$$\tau_{ij} = \mu \left(\frac{\partial u_i}{\partial x_j} + \frac{\partial u_j}{\partial x_i} \right) - \mu \frac{2}{3} \frac{\partial u_k}{\partial x_k} \delta_{ij}, \quad (2.3)$$

where μ is the dynamic viscosity. Assuming no body forces, the momentum equations become

$$\frac{\partial \rho u_i}{\partial t} + \frac{\partial \rho u_i u_j}{\partial x_j} = -\frac{\partial p}{\partial x_i} + \frac{\partial}{\partial x_j} \left[-\frac{2}{3} \mu \frac{\partial u_k}{\partial x_k} \delta_{ij} + \mu \left(\frac{\partial u_i}{\partial x_j} + \frac{\partial u_j}{\partial x_i} \right) \right]. \quad (2.4)$$

The viscosity is determined through the Sutherland's law

$$\frac{\mu(T)}{\mu_j} = \left(\frac{T}{T_j} \right)^{3/2} \frac{T_j + S_0}{T + S_0}, \quad (2.5)$$

where T is the local temperature and j -indices denote the jet reference condition¹. For the wall-jets, a reference temperature of $S_0 = 110.4K$ valid for air at moderate temperatures and pressures is used.

2.1.2. Conservation of energy

The energy conservation equation needs the most attention since many different forms exist. Here we use the governing equation for the total non-chemical energy, the sum of the internal and kinetic energy per unit mass $E = e + \frac{1}{2}u_i u_i$, which reads

$$\frac{\partial \rho E}{\partial t} + \frac{\partial \rho E u_j}{\partial x_j} = \dot{\omega}_T - \frac{\partial q_i}{\partial x_i} + \frac{\partial (u_i (\tau_{ij} - p \delta_{ij}))}{\partial x_j} + \dot{Q} + \rho \sum_{k=1}^n \theta_k f_{k,i} (u_i + V_{k,i}). \quad (2.6)$$

Here, $\dot{\omega}_T$ is the heat release term due to combustion and \dot{Q} is the heat added by external sources (e.g. an electric spark) and $V_{k,i}$ is the x_i -component of the diffusion velocity of k th species θ_k . The last term on the right hand side describes the power produced by a volume force $f_{k,i}$. The summation convention over repeated indices is used. The heat fluxes q_i are approximated by Fourier's law $q_i = -\lambda \frac{\partial T}{\partial x_i}$, where λ is the coefficient of thermal conductivity and T is the temperature.

Assuming no external forces and no external heat sources in the flow and using Fourier's law the governing equation for the total energy is simplified to

$$\frac{\partial \rho E}{\partial t} + \frac{\partial \rho E u_j}{\partial x_j} = \dot{\omega}_T + \frac{\partial}{\partial x_j} \left(\lambda \frac{\partial T}{\partial x_j} \right) + \frac{\partial (u_i (\tau_{ij} - p \delta_{ij}))}{\partial x_j}. \quad (2.7)$$

We assume a thermally perfect gas, and therefore the internal energy and enthalpy are only functions of temperature,

$$\begin{aligned} e = e(T) &\implies de = c_v dT \\ h = h(T) &\implies dh = c_p dT. \end{aligned} \quad (2.8)$$

Here, c_v and c_p are the specific heats at constant volume and pressure respectively, which in general are functions of the temperature. If the specific heats are also assumed constant, the system is calorically perfect and

$$\begin{aligned} e &= c_v T \\ h &= c_p T. \end{aligned} \quad (2.9)$$

The gas is assumed to be ideal and to obey the perfect gas law

$$p = \rho R T, \quad (2.10)$$

¹Not to be confused with the dummy index j in other equations.

where R is the specific gas constant. Using the definition of enthalpy and the perfect gas law, the specific heats can be expressed as

$$\begin{aligned} c_p &= \frac{\gamma R}{\gamma - 1} \\ c_v &= \frac{R}{\gamma - 1}, \end{aligned} \quad (2.11)$$

where $\gamma = c_p/c_v$. Using these relations, the pressure and temperature can be written as functions of the internal energy e

$$\begin{aligned} p &= \rho RT = \rho R \frac{e}{c_v} = (\gamma - 1)\rho e \\ T &= \frac{p}{\rho R} = \frac{(\gamma - 1)}{R} e. \end{aligned} \quad (2.12)$$

The heat diffusion can be expressed as a function of the inner energy and the specific heat c_p using (2.12) and (2.11) as

$$q_j = -\lambda \frac{\partial}{\partial x_j} \left(\frac{(\gamma - 1)e}{R} \right) = -\lambda \frac{\partial}{\partial x_j} \left(\frac{\gamma e}{c_p} \right). \quad (2.13)$$

Here, constant values of c_p , c_v and γ are considered. The heat diffusion is often defined in terms of the Prandtl number, relating the momentum and heat transport

$$Pr = \frac{\nu}{\lambda/(\rho c_p)} = \frac{\mu c_p}{\lambda}. \quad (2.14)$$

Using this definition, the energy flux can be expressed as

$$q_j = -\frac{\gamma \mu}{Pr} \frac{\partial e}{\partial x_j} \quad (2.15)$$

and the energy equation, in terms of $E_t = \rho E$, for an ideal gas becomes

$$\frac{\partial E_t}{\partial t} + \frac{\partial E_t u_j}{\partial x_j} = \dot{\omega}_T + \frac{\partial}{\partial x_j} \left[\frac{\gamma \mu}{Pr} \frac{\partial}{\partial x_j} \left(\frac{E_t}{\rho} - \frac{1}{2} u_i u_i \right) \right] + \frac{\partial (u_i (\tau_{ij} - p \delta_{ij}))}{\partial x_j}. \quad (2.16)$$

2.1.3. Conservation of species mass

A convenient approach for the species conservation is to utilize the species mass fractions of the mixture defined by

$$\theta_k = \frac{m_k}{m} = \frac{\rho_k}{\rho}, \quad (2.17)$$

where m_k is the mass of the species k in a given volume V and m is the total mass in this volume. Each of the species k involved in the flow obeys a mass transport equation of the form

$$\frac{\partial \rho \theta_k}{\partial t} + \frac{\partial}{\partial x_i} [\rho \theta_k (u_i + V_{k,i})] + \dot{\omega}_k = 0, \quad (2.18)$$

where $V_{k,i}$ θ_k is the diffusive flux in the i -direction, and $\dot{\omega}_k$ is the mass reaction rate describing the rate of creation or destruction of the species. Diffusive fluxes are caused by a number of transport processes on the molecular level.

Accounting for all these is often computationally too expensive. The most common approximation is to assume that the fluxes follow the Fick's law

$$V_{k,i}\theta_k = -\mathcal{D}_k \frac{\partial \theta_k}{\partial x_i}, \quad (2.19)$$

where \mathcal{D}_k is the binary diffusion coefficient of species k . Using this approximation, the species conservation equation takes the form

$$\frac{\partial \rho \theta_k}{\partial t} + \frac{\partial}{\partial x_j} (\rho \theta_k u_j) = \frac{\partial}{\partial x_j} \left(\rho \mathcal{D}_k \frac{\partial \theta_k}{\partial x_j} \right) + \dot{\omega}_k, \quad (2.20)$$

where θ_k and $\dot{\omega}_k$ are the mass fractions and the reaction rate of the oxidizer, fuel and passive scalar species. An equal diffusion coefficient, \mathcal{D}_k , for all scalars is used to approximate the diffusive fluxes. The \mathcal{D}_k coefficients are often characterized in terms of the Lewis number, $Le_k = \frac{\lambda}{\rho C_p \mathcal{D}_k}$.

2.2. Chemical reaction

Our knowledge about the gas reactions in general and the combustion of fuels in particular has substantially improved. There is a large body of publications about elementary reaction mechanisms and their rate data. From a ‘‘chemist’’ point of view, a simplified reaction model can consist of a hundred reactions and more than twenty species. For instance, a mechanism for methane oxidation comprises 77 reactions and 49 species. However, there are a lot of different methods to reduce the number of independent variables in a mechanism, and a lot of efforts have been undertaken to develop reduced mechanisms for fuel combustion. The reduced mechanisms are very useful for numerical simulation purposes, as they decrease the amount of data storage requirements and computational resources required. Nonetheless, in the numerical simulations with fluid dynamical aspects a single step global reaction is often used. A single-step global reaction is only a coarse approximation of the chemistry occurring in real life, even for simple chemical reactions, but it allows us to study the interactions between heat-release and turbulence in a real three-dimensional flow. It is a very useful methodology to gain insight into the generic characteristics and effects of a chemical mechanism in different flow fields. Using DNS together with the simple chemistry has been a customary approach to address combustion problems and it has been frequently used to study different flow fields.

2.2.1. Single-step irreversible chemical reaction

A single-step reaction involving N species can be described by



where \mathcal{M}_k denotes the concentration of species k in moles per unit volume, ν_k^r are the stoichiometric coefficients of the reactants and ν_k^p are the stoichiometric coefficients of the products. Consider a simple case where reaction involves only

the oxidizer species O and fuel species F that react to form a product P which is described as



The mass fraction θ_k of each species (O , F and P) follows the governing equations described by eq. (2.20) and thus, it implies that the reaction mass rates of the species are linearly related as

$$\dot{\omega}_f = \frac{1}{r} \dot{\omega}_o = -\frac{1}{r+1} \dot{\omega}_p. \quad (2.23)$$

An Arrhenius-type reaction rate and $r = 1$ is assumed. The source term in the fuel species concentration equation reads

$$\dot{\omega}_f = -k_r \rho^2 \theta_o \theta_f \exp(-Ze/T), \quad (2.24)$$

where $Ze = E_a/RT_j$ is the Zeldovich number and k_r is the reaction rate constant. The exponential term is the Boltzmann factor which from kinetic theory can be seen to give the fraction of all collisions that have greater energy than the activation energy. The pre-exponential factor is the collision frequency, and can be further rewritten with the aid of the non-dimensional Damköhler number, $Da = \frac{h}{U_j} k_r \rho_j$, where h is a characteristic length scale. The definition of the Damköhler number will be further explained in the following section.

A further simplified reaction term can be considered which is a function of density and reactant concentrations and does not depend on temperature,

$$\dot{\omega}_f = -k_r \rho^2 \theta_o \theta_f. \quad (2.25)$$

The combustion heat release term, $\dot{\omega}_T$, in the energy equation, eq. (2.16), is related to the species reaction rate terms by

$$\dot{\omega}_T = -\sum_{k=1}^N \Delta h_{f,k}^0 \dot{\omega}_k, \quad (2.26)$$

where $\Delta h_{f,k}^0$ is the formation enthalpy of the k^{th} -species. Due to the linear relation between different reaction-rate terms, see eq. (2.23), $\dot{\omega}_T$ is formulated as

$$\dot{\omega}_T = \frac{Ce}{(\gamma - 1)M_0^2} e_0 \dot{\omega}_p, \quad (2.27)$$

where M_0 is the inlet-based Mach number and Ce is the non-dimensional heat release parameter and e_0 is a characteristic measure of the internal energy, e .

2.3. Important non-dimensional numbers

Reynolds number

The Reynolds number Re is a dimensionless number that gives a measure of the ratio of inertial forces to viscous forces and in a general sense, gives an indication for the strength of the turbulence. However, characteristic velocity and length scales should be used for deduction of meaningful information. In chemically reacting flows, when a substantial amount of heat is released, the local temperature and density of the fluid significantly vary, which result in

wide ranges of local Reynolds numbers. It is common to report the cold-flow Reynolds number, with properties of the fluid before chemical reaction occurs. Here, the inlet Reynolds number is defined as

$$Re = \frac{U_j h}{\nu_j}, \quad (2.28)$$

where h is the jet inlet height and j is used to denote properties at the inlet jet center.

Mach number

The Mach number M is the speed of an object moving through air, or any other fluid substance, divided by the speed of sound in that fluid for the particular physical conditions, including the temperature and pressure. Here, the inlet Mach number is defined as

$$M = \frac{U_j}{a}, \quad (2.29)$$

where $a = \sqrt{\gamma RT}$. In this study, the simulations are performed in subsonic speeds, $M < 1$ and the numerical values are specified for each case.

Prandtl number

The Prandtl number Pr is a dimensionless number, that is the ratio of momentum diffusivity or kinematic viscosity to thermal diffusivity. It is defined as

$$Pr = \frac{\nu}{\alpha} = \frac{\mu c_p}{\lambda}, \quad (2.30)$$

where ν is the kinematic viscosity, α is the thermal diffusivity and λ is the thermal conductivity. Note that contrary to the Reynolds number, the Prandtl number contains no length scale in its definition and is dependent only on the fluid state. Prandtl number is used to relate the momentum to heat transport properties and can be found in property tables for different fluids.

Lewis number

Lewis number is a dimensionless number defined as the ratio of thermal diffusivity to mass diffusivity and can be expressed as

$$Le_k = \frac{\lambda}{\rho C_p \mathcal{D}_k}, \quad (2.31)$$

where λ is the thermal diffusivity and \mathcal{D}_k is the mass diffusion coefficient.

Schmidt number

The Schmidt number is a dimensionless number defined as the ratio of momentum diffusivity or viscosity and mass diffusivity. The Schmidt number, Sc_k compares momentum and molecular diffusion of species k and is defined as

$$Sc_k = \frac{\mu}{\rho \mathcal{D}_k} = Pr Le_k. \quad (2.32)$$

In this study, the Schmidt number is constant and equal to the Prandtl number for all species, which implies a unity assumption of the Lewis number.

Damköhler number

The Damköhler number Da is a dimensionless number used to relate the chemical reaction time scale to a representative time scale of the flow. Various definitions may be found in the literature for the Damköhler number. The general definition of the Damköhler number is

$$Da = \frac{\tau_{\text{conv}}}{\tau_{\text{react}}} = \frac{h}{U_j} \bar{k}_r \rho_j. \quad (2.33)$$

The flame structure and the combustion regime depend on the chemical characteristic time, τ_{react} . For fast chemistry, (low τ_{react} values and high Damköhler numbers), the flame is very thin. For larger values of the chemical time scale, the flame thickness becomes larger and of the same order as the Kolmogorov length scale, η_k .

Karlowitz number

The Karlowitz number is defined as the ratio of the chemical time scale to the Kolmogorov time scale,

$$Ka = \frac{\tau_{\text{react}}}{\tau_{\text{Kolmogorov}}}. \quad (2.34)$$

For premixed combustion, the interactions between the turbulence and the chemistry can be measured by the Karlowitz number.

Zeldovich number

Activation energy of a chemical reaction is the energy the reactants must acquire before they can react. In practice, the activation energy is determined experimentally, for each particular reaction. The Zeldovich number, is a non-dimensional measure of the temperature sensitivity of the reaction rate, and here it is defined in terms of the jet inlet temperature, T_j as

$$Ze = \frac{E_a}{R T_j} = \frac{T_a}{T_j}. \quad (2.35)$$

Note that the Zeldovich number may be defined as the product of the temperature rise $\alpha = (T_\infty - T_0)/T_\infty$ and the non-dimensional activation energy $E_a R/T_\infty$, however, for the numerical values of the Zeldovich number, we have used the definition in eq. (2.35) throughout this work.

Non-dimensional heat release parameter

The non-dimensional heat release parameter, Ce is defined as

$$Ce = \frac{-H^0}{c_p T_j}, \quad (2.36)$$

where, $-H^0$ is the heat of reaction for the overall chemical reaction.

2.4. Averaging principles

Consider the dynamic quantity $f(x, t)$, which could represent, e.g. temperature, the concentration of chemical species, or a component of velocity. Here x is the vector denoting the spatial coordinates and t is time. The Reynolds average of f , denoted by \overline{f} , can be defined as an ensemble, spatial, and/or temporal average, depending on the problem. It is often convenient to use the Reynolds decomposition

$$f = \overline{f} + f',$$

where f' is the fluctuation about the mean. In the case of variable density flows one can alternatively use density-weighted or Favre-averaged values, denoted by \tilde{f}

$$\tilde{f} = \overline{\rho f} / \bar{\rho},$$

where $\rho(x, t)$ is the fluid density. If Favre averaging is used, f is decomposed as

$$f = \tilde{f} + f'',$$

where f'' is the fluctuation about the density-weighted average and \tilde{f} denotes the mass-weighted mean.

Simulations of non-premixed combustion

3.1. Combustion simulation overview

Performing any kind of turbulent combustion simulation is a challenging task for various different reasons. Combustion has a strong multi-scale and non-linear nature and a wide range of length and time scales are involved which add to the broad spectrum of turbulence scales. In addition, large numbers of species are involved in any reacting flow even in the simplest combustion processes, bringing further complexity to the problem. Besides, combustion processes in real world situations usually occur in multiphase environments, with presence of thermal radiation and acoustic effects. Moreover, all these different phenomena are interacting with each other and tight couplings exist between them, see e.g. Hawkes *et al.* (2007). Therefore, in simulations of reacting flows, some types of simplifications need to be done. Depending on the priorities and the important issues, these simplifications may be done for the flow aspects or for the chemistry involved. The description of the reactions, however, almost always has to be simplified. For instance, a complete mechanism for the simple reaction of hydrogen and oxygen gases typically involves 19 reactions and 9 species (Conaire *et al.* 2004). Many different numerical efforts have been undertaken, and several simulations of turbulent combustion have been performed. Numerous combustion models have been developed and used for various applications. However, industrial combustion systems are constantly changing and the next generation of combustion systems are likely to operate in previously unexplored regimes. Internal combustion engines and gas turbines may burn fuel at lower temperatures, higher levels of dilution and much less pollutant emissions. The reaction process in these new environments brings up complicated challenges. The new models are expected to predict much wider ranges of turbulent combustion regimes and of course be more accurate. Therefore, better understanding of the fundamentals of combustion systems, in particular “turbulence-chemistry” interaction, seems to be necessary for achieving efficient burnings. Bilger (2000) presented an overview of the issues of rather recent research interests in the turbulent combustion, computational and modeling community. The application of detailed chemistry and transport models was reviewed and discussed by Hilbert *et al.* (2004).

There are a number of different ways to solve the governing equations and to deal with turbulent combustion problems numerically. The Reynolds averaged

Navier-Stokes (RANS) approach starts with ensemble averaging the governing equations, in which the Reynolds decomposition is used. The turbulence is described through the turbulent stresses and thus information will be provided about the averaged quantities. Large eddy simulation (LES) is an intermediate tool for computing turbulent flows. In LES, the large scales of turbulent flow are resolved and the small scales of the flow are modeled, using the information obtained from the resolved field. Unlike RANS techniques, LES provides a more realistic and rather detailed data analysis possibility, which gives some knowledge about different structures of turbulent flows. See Fureby (2008), for a recent review of LES applications in engineering problems. Indeed, LES is a very useful tool for turbulent flow computations in particular when no reaction is involved and modeling issues are restricted to those of the small scales of turbulence. The most accurate computational tool is the direct numerical simulation (DNS), which solves all the flow equations without making any further assumptions, resolves all the scales from large integral scales down to small Kolmogorov scales of the flow and even the fine structures of the flame. In turbulent combustion flows, both the time and space resolution requirements for DNS are more restricted than what is required for the non-reacting counterpart flows, thus it may be very expensive to perform a DNS of real-size problems. For instance, for a reaction with high Damköhler number, flame becomes thin and therefore much finer grid resolution is needed. However, DNS provides detailed information about different mixing and reaction interactions in the turbulent flow field and thus paves the way for development of new accurate combustion models. DNS data are often used for validation of combustion models but in addition to that, thorough fundamental insight of the various aspects of the physical problem can be gained through a careful analysis of the data.

3.1.1. *DNS of turbulent reactive flows*

In the past three decades, DNS has become an essential tool to understand and model turbulent combustion. DNS, numerically solves the set of equations describing turbulent flames by resolving all chemical and flow scales, (Vervisch & Poinso 1998). Increasing computational resources have facilitated high-resolution simulations (Chen 2011) and also simulation of more complex phenomena including that of fluid dynamics coupled with reactions using detailed chemistry. An example is a reacting flow simulation performed by Knaus & Pantano (2009) to study the effect of heat release in shear layers.

DNS investigations are beneficial in mixing and combustion applications, for the fact that they provide access to the complete solution. All length and time scales are resolved and the statistics of higher order, such as correlations, probability density functions and dissipation rates can therefore be computed anywhere in the computational domain. Due to the computational restrictions

which are still present¹, the DNS studies are mostly dedicated to the canonical flow fields rather than the real engineering applications. However, DNS provides physical insights into chemistry-turbulent interactions, which in turn will help to improve the combustion models that can handle the engineering-level calculations.

The progress in the application of DNS to study turbulent premixed and non-premixed combustion has been reviewed by Poinso *et al.* (1996) and Vervisch & Poinso (1998). The available literature on DNS of reacting flows and rather recent research capabilities of DNS is reviewed by Westbrook *et al.* (2005). A thorough review of DNS of reacting flow may be found in Vervisch (2000) and also in the recent paper by Chen (2011).

Here, the detailed review of recent DNS of reacting flows will not be included, instead, the related articles will be mentioned in each paper separately, when they are being used and are related to the topic under discussion.

3.1.2. DNS of flame-wall interaction

Many combustion applications in confined domains contain regions where mixing and reaction take place close to a wall. Thus, better understanding of the wall effects plays an essential role in gaining insight into the full problem.

Most of the DNS of reacting flow studies have excluded the wall effects. In cases with wall interactions, a closer look at the fundamental statistics seems to be necessary. However, the numerical investigations of wall-bounded reacting flows have often been restricted to the case of turbulent boundary layers and turbulent channel flows, see Ruetsch *et al.* (1995). A recent example is the work by Gruber *et al.* (2010), who investigated the turbulent flame-wall interaction in a channel flow.

These studies have produced important insight, but much more remains to be studied in the area of wall-bounded turbulent combustion. Poinso *et al.* (1993) studied flame-wall interaction of laminar and premixed combustion using compressible two-dimensional DNS and a simple reaction. Bruneaux *et al.* (1996) performed incompressible three-dimensional simulations of premixed combustion in a channel using a simple reaction. They found that quenching distances decrease and maximum heat fluxes increase in comparison to those of laminar flames. Their DNS data were also used by Bruneaux *et al.* (1997) to develop and evaluate a flame surface density model. Using a complex reaction mechanism consisting of 18 reactions involving 8 species, one-dimensional premixed and non-premixed flame interaction with an inert wall was simulated by Dabrieau *et al.* (2003). Wang & Trouvé (2006) used DNS to study flame structure and extinction events of non-premixed flames interacting with a cold

¹Despite the enormous progress in recent years in the availability of computational resources, e.g. PRACE infrastructure in Europe, <http://www.prace-ri.eu>,

wall. Their simulation was fully compressible, two-dimensional and the reaction was described using a single-step model containing four species.

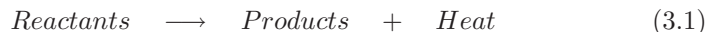
3.2. Combustion modeling

The understanding and prediction of the behavior of turbulent reacting flows is generally much more difficult than for non-reacting flows. These difficulties arise for different reasons, the most common is the compressibility effects, which make it necessary to solve the conservation of energy equation beside mass and momentum equations. Next, reacting flows in general include heat release and significant density fluctuations and this has implications for the averaging of the governing equations. The mean heat-release rate is one of the main quantities that needs to be approximated in combustion modeling and is often of important practical interest. Moreover, conservation equations for chemical species must be included. Furthermore, turbulent combustion systems involve multiple phases which adds to the complexity of modeling issues, see Veynante & Vervisch (2002), Riley (1998) or Vervisch & Veynante (2011) for an introduction to combustion modeling.

3.3. Premixed and non-premixed combustion modeling

Two classifications of reactions are generally used in turbulent combustion, which simplify the problem particularly in development and utilization of models, namely premixed and non-premixed. The latter is the reaction between a premixed fuel and oxidant which are locally ignited by means of a spark, a common example is the internal combustion engine. The ignition starts the flame which propagates through the mixture and generates hot products. In the non-premixed regime the fuel and oxidizer are introduced separately, for example a fuel jet which is injected into air. Chemical reaction can occur as the fuel and oxidant mix locally at the molecular level. Therefore the flame can exist where the fuel and oxidant are mixed locally and the reaction depends on the mixing rate, at least to some extent. Finally, reactions can also occur when the species are partially premixed. For example, in the problem of a fuel jet into air, it is possible for the fuel and air to mix somewhat before ignition occurs.

If we consider a simplified one-step irreversible premixed chemical reaction,



we can describe the flame using a *progress variable* c , such that $c = 0$ in the fresh gases and $c = 1$ in the fully burned ones. This progress variable may be defined using temperature or the mass fractions

$$c = \frac{T - T_u}{T_b - T_u} \quad \text{or} \quad c = \frac{\theta_f - \theta_f^u}{\theta_f^b - \theta_f^u}. \quad (3.2)$$

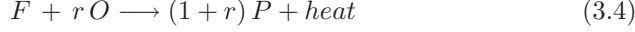
Here, T , T_u and T_b are the local temperature, the unburned temperature and the burned gases temperatures respectively; and accordingly θ_f , θ_f^u and θ_f^b are

the local, unburned gases and burned gases fuel mass fractions. Assuming the same molecular and thermal diffusivities, unity Lewis number, without heat losses or compressibility effects, then the two definitions are equivalent and mass and energy balance equations reduce to a single balance equation for the progress variable,

$$\frac{\partial \rho c}{\partial t} + \frac{\partial}{\partial x_j} (\rho c u_j) = \frac{\partial}{\partial x_j} \left(\rho \mathcal{D} \frac{\partial c}{\partial x_j} \right) - \dot{\omega}. \quad (3.3)$$

This equation describes the displacement of the c -isosurfaces.

For the non-premixed case, we can consider an irreversible one-step chemical reaction as,



where r is the stoichiometric coefficient. The mixture fraction Z is defined as

$$Z = \frac{\phi \frac{\theta_f}{\theta_{f,0}} - \frac{\theta_o}{\theta_{o,0}} + 1}{\phi + 1} = \frac{r \theta_f - \theta_o + \theta_{o,0}}{r \theta_{f,0} + \theta_{o,0}}, \quad (3.5)$$

where $\theta_{f,0}$ is the fuel mass fraction in the fuel stream, $\theta_{o,0}$ is the oxidizer mass fraction in the oxidizer stream and ϕ is the equivalence ratio of the non-premixed flame

$$\phi = \frac{r \theta_{f,0}}{\theta_{o,0}}. \quad (3.6)$$

The mixture fraction obeys the balance equation,

$$\frac{\partial \rho Z}{\partial t} + \frac{\partial}{\partial x_j} (\rho Z u_j) = \frac{\partial}{\partial x_j} \left(\rho \mathcal{D} \frac{\partial Z}{\partial x_j} \right), \quad (3.7)$$

which does not include a source term. An important value of Z is its stoichiometric value, Z_{st} , which is obtained when fuel and oxidizer are in the stoichiometric condition, i.e. $r \theta_f = \theta_o$. Thus the stoichiometric mixture fraction is

$$Z_{st} = \frac{\theta_{o,0}}{r \theta_{f,0} + \theta_{o,0}} = \frac{1}{r \phi + 1}. \quad (3.8)$$

3.4. Non-premixed combustion modeling tools

In this section, we will go briefly through some basic tools in non-premixed combustion modeling. Though, nor the modeling in general, neither the non-premixed combustion modeling in particular, are included directly as part of our study, we here give a brief background of them. An important practice is to implement our state-of-the-art knowledge, gained from DNS studies, into the models. We can of course get a lot of important and useful information from our direct simulations, however, learning the physics behind them in order to improve the models is not a trivial task.

The mean heat release rate is one of the main quantities of practical interest that should be approximated by a turbulent combustion model. The simplest and more direct approach is to develop the chemical rate in Taylor series as function of species mass fractions and temperatures. To understand

the basic difficulty of applying averaging methods to reacting flows, consider the approximately constant density, one step Arrhenius-type reaction obeying eq. (3.4). Here, one unit of mass of fuel F combines with r units of mass of oxidizer, O to produce $(1+r)$ units of mass of products P in addition to heat, the fuel reaction rate is approximately given

$$\dot{w}_F = -A \rho^2 \theta_F \theta_O e^{(-E_a/RT)}. \quad (3.9)$$

Here, A is a rate constant which is usually called the pre-exponential factor in the Arrhenius expression, T is the fluid temperature and E_a is the activation energy of the reaction, see Riley (1998). Assuming a constant density ρ , the conservation equation (3.3) for fuel reads

$$\frac{\partial \theta_F}{\partial t} + \frac{\partial}{\partial x_j} (u_j \theta_F) = \frac{\partial}{\partial x_j} \left(\mathcal{D} \frac{\partial \theta_F}{\partial x_j} \right) - \rho \theta_F \theta_O A e^{(-T_a/T)}, \quad (3.10)$$

where $T_a = E_a/R$ is the activation temperature. Averaging eq. (3.10) gives

$$\frac{\partial \overline{\theta_F}}{\partial t} + \overline{u_j} \frac{\partial \overline{\theta_F}}{\partial x_j} = \frac{\partial}{\partial x_j} \left(\overline{\mathcal{D} \frac{\partial \theta_F}{\partial x_j}} \right) - \frac{\partial}{\partial x_j} \overline{(u_j' \theta_F')} - \overline{\rho \theta_F \theta_O A e^{(-T_a/T)}}. \quad (3.11)$$

Two unclosed terms appear after the averaging procedure, one is $\overline{(u_j' \theta_F')}$ which is similar to the Reynolds shear stress term in the averaged momentum equation, and can be modeled in a similar manner. The second term, namely $\overline{\rho \theta_F \theta_O A e^{(-T_a/T)}}$, is the average of the reaction rate term, which is the root of the essential difficulties. Often, for example in non-premixed reaction, the flame zone is very thin. Thus, flow consists of regions of either fuel or oxidizer species, with very little overlap and high segregation, i.e. $\theta_F \theta_O \ll \overline{\theta_F} \overline{\theta_O}$. Note that, this type of averaging approach for the cases with $T \approx const.$, is used for chemical engineering problems, however, if $T \neq const.$, one needs to expand the exponents in the form of a Taylor series. Understandably, even for small temperature fluctuations, the modeling will become very difficult. If higher order correlations of $1/T$ and the species mass fractions all need to be modeled accurately, which is generally not feasible, so some other tools are used in turbulent combustion modeling.

3.4.1. Geometrical approach: flame surface analysis

In this approach, the flame front is described as a geometrical entity. Here, the analysis is generally linked to the assumption of a sufficiently thin flame, viewed as an interface between fresh and burned gases in premixed combustion or as an interface between fuel and oxidizer in non-premixed cases. Two formalisms are usually proposed within this framework: G -field equation and flame surface density concept.

The G -equation model proposed by Williams (1985), uses an iso-surface method to describe the evolution of the flame front as an interface between the unburned and burned gases. The function G is a scalar field defined such that

the flame front position is at $G = G_0$ and that G is negative in the unburned mixture. The instantaneous and local G -equation can be derived by considering the instantaneous flame surface. We will not discuss the details of this method any further in the present study.

In flame surface density description, the flame is identified as a surface and the flame surface density Σ is introduced. As the flame propagates normal to itself, the mean burning rate is directly proportional to the flame surface area.

3.4.2. *Statistical approach: probability density function*

Prediction of radicals, intermediate species and pollutants requires knowledge of the flame internal structure, for the intermediate states between fresh and burned gases in premixed flames or between fuel and oxidizer in non-premixed flames. Despite the fact that, in the G -field equation or in the flame surface density Σ approaches, some statistical treatment is performed, but they are based on the geometrical view of the flame as a thin interface. In probability density function (PDF) methods, this assumption is relaxed and one can focus on the statistical characteristics of the flame, throughout intermediate states of the flame and different regions of the flow, see O'Brien (1980), Pope (1985) and Dopazo (1994).

Considering a non-premixed flame where the chemistry is reduced to a single-step reaction and the radiative heat losses are neglected. Laminar combustion may be parameterized with two variables, for instance, fuel mass fraction, θ_F and mixture fraction Z . The turbulent flame is then fully described by the joint probability density function of mixture fraction and fuel mass fraction, $\overline{P}(\theta_f, Z; x, t)$. For such flames, it is interesting to focus on the statistical properties of the fuel mass fraction, θ_f for a given value of the mixture fraction Z . According to Vervisch & Veynante (2011), two main directions may be chosen to build numerical models from PDF. One is to presume the PDF shape from the available mean quantities and the other is to solve a balance equation for the PDF.

3.4.3. *Mixture fraction approach: small scales analysis*

Turbulent mixing can be used as a measure for quantifying the burning rate. In case of a large Damköhler number, which is a common assumption in combustion modeling, the reaction rate is limited by turbulent mixing and it may be described in terms of the scalar dissipation rate. Peters (2000) defines flamelets as "thin diffusion layers embedded in a turbulent non-reactive flow field". This thin region is assumed to be smaller than Kolmogorov length scale and therefore the region is locally laminar. The flame surface is defined as an iso-surface of the mixture fraction, Z in non-premixed combustion. In non-premixed flames, fresh fuel and fresh oxidizer need to be mixed at the molecular level for reaction

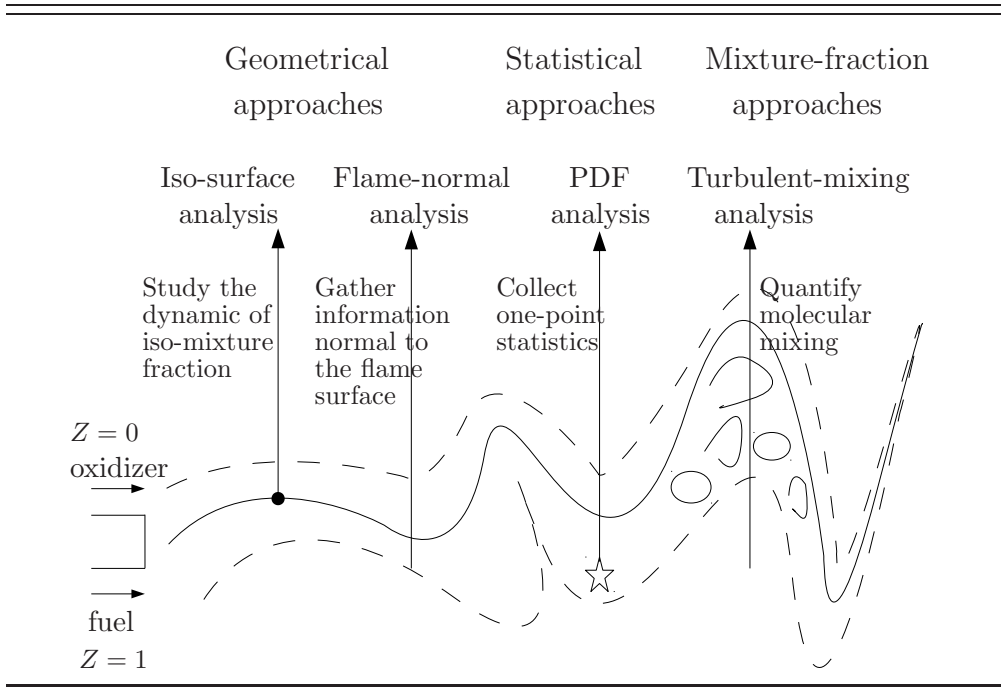


FIGURE 3.1. Schematic of different combustion modeling approaches

to take place and the flame is mainly controlled by turbulent mixing occurring between the two gas streams. If we assume equal molecular diffusivities for all chemical species, the mixture fraction, Z can be defined as the local mass fraction of a conserved scalar originating in the fuel stream. In the case of infinite rate or equilibrium chemistry, the concentrations of the various chemical species can be functionally related to the mixture fraction, enabling the average concentrations to be expressed in terms of these relationships and the probability density of the mixture fraction. For finite-rate chemistry, theories have been developed relating the average concentrations to the joint probability density of Z and its dissipation rate χ . The scalar dissipation rate χ , provides a direct measure for the decay speed of the fluctuations, Veynante & Vervisch (2002).

3.4.4. *Non-premixed combustion modeling issues*

In previous sections, the major important tools which are used in turbulent combustion modeling were introduced briefly. The three most useful quantities for description of a turbulent flame were introduced, namely, the scalar dissipation rate, the probability density functions and the flame surface density. A

schematic of different types of modeling tools for non-premixed combustion is presented in figure 3.1². Interestingly, all these quantities are associated with each other and the links between them have been developed. The exact relation between the mean scalar dissipation rate, probability density function and the generalized flame surface density may be found in Veynante & Vervisch (2002). These relations show that the scalar dissipation rate is a key quantity that directly or indirectly relates different tools to each other. Thus, studying its behavior throughout the simulation field is of prominent importance. Having access to full range of scales, provided by DNS data analysis, we can focus on the characteristics of these essential quantities everywhere in the domain, including their near-wall behavior.

²This figure is originally generated by the author for the purpose of present work, however, it has the spirit of a similar figure in the paper by Vervisch (2000).

Turbulent wall-jet

4.1. Wall-jet set-up and background

A wide range of flows have been described using the terminology “wall-jet”, all sharing a common characteristic, that the outer part of these flows behaves similar to a jet flow and the inner part behaves more or less like a boundary layer flow. A wall-jet is formed, when a jet flow evolves over a flat surface in the absence or presence of an external stream. Depending on the type of the jet, its injection direction, the nozzle geometry and the wall boundary conditions, such as the surface temperature or roughness, many different kinds of wall-jet flows may form. A few examples are, two-dimensional planar wall-jets, studied by Conlon & Lichter (1995), the coflow wall-jets, Coanda wall-jets (wall-jets on curved surfaces), investigated by Neuendorf & Wygnanski (1999), three-dimensional wall-jets addressed by Hall & Ewing (2010) and different kinds of impinging jets.

The turbulent wall-jet includes a number of interesting fluid mechanics phenomena with close resemblance to many engineering applications. Wall-jets are widely used for boundary layer control, cooling of turbine blades, and to either enhance or reduce the convective wall heat-transfer. Impinging wall-jets have applications in heating or annealing of metal, plastic or glass during the manufacturing process, where this technique is used to control the processing temperature. Wall-jets are also formed when fuel is injected into internal combustion engines. Sometimes, wall-jets are injected parallel to the inner surface of a combustion chamber to protect it from the hot products. In supersonic aeronautical applications, wall-jet occurs when fuel is injected into the boundary layer for drag reduction purposes.

The “wall-jet” flow was addressed by Glauert (1956), where the term was initially used, though, this was not the first work on wall-jets, but perhaps the first one solely dedicated to the subject. One of the earliest known works on wall-jets is an experimental study by Förthmann (1934), in which he extended his research on jet flows to jets close to a surface. Since the 60’s, numerous experimental, theoretical and some numerical studies have been performed on different kinds of wall-jets. A comprehensive review on turbulent wall-jet experiments prior to 1980 can be found in Launder & Rodi (1981), a few of which are mentioned below. Förthmann (1934) observed the self-preserving nature of

the wall-jet, and that the boundary-layer thickness varies linearly with downstream position, x , and that the maximum velocity varies as $x^{-1/2}$. Glauert (1956) was maybe the first to divide the flow into an inner and an outer part on either side of the maximum velocity and treated the two regions separately. In many studies, particular attention has been paid to the appropriate similarities in different regions of the wall-jet flow and the corresponding velocity and length scales. Narashima *et al.* (1973) suggested that the mean flow parameters should scale with the jet momentum flux and the kinematic viscosity. The same approach was employed by Wygnanski *et al.* (1992) in an effort to remove inlet Reynolds number dependency and to determine the skin friction from the decrease in the momentum flux; see also Zhou *et al.* (1996). George *et al.* (2000) performed a similarity analysis of the inner and outer part of the wall-jet without coflow, using different experimental data of previous studies. Parallel to the analytical works on the similarity characteristics of the wall-jet flow, experimental work was initiated by Bradshaw & Gee (1960). They performed measurements of a turbulent wall-jet and reported that the turbulent shear stress attains a finite value at the point of maximum velocity. Eriksson *et al.* (1998) studied a wall-jet in a large water tank and used Laser Doppler Velocimetry for their measurements. Recently, an experimental study on plane wall jets was reported by Dey *et al.* (2010) in which, they investigated the effects of suction and injection from the wall.

Although experimental and theoretical studies on the wall-jet flows have been numerous in the past, the numerical research has remained limited. Accurate numerical data can indeed, strengthen conclusions on scaling and similarity and also provide closer insight into the development of the jet, including transitional features. However, performing a numerical simulation of the spatially developing turbulent wall-jet flow is computationally expensive, thus, reports on simulations of the wall-jet flow are scarce. The very early computational studies of the plane turbulent wall-jet, using RANS modeling, are included in the review by Launder & Rodi (1981). Dejoan & Leschziner (2005) performed a well-resolved large eddy simulation and compared the results with the experiments by Eriksson *et al.* (1998). The results agreed well with the experiments for the velocities and the Reynolds stresses. Wernz & Fasel (1996, 1997) employed DNS to investigate instability mechanisms in a transitional wall-jet. The breakdown of a finite-aspect-ratio wall-jet was studied by Visbal *et al.* (1998). Levin *et al.* (2005) studied the laminar breakdown of a wall-jet using linear stability analysis and DNS. Gogineni *et al.* (1999) studied transitional two-dimensional wall-jets at a low Reynolds number.

Ahlman *et al.* (2007) reported the first DNS of a turbulent wall-jet flow, including the scalar mixing. This was followed by another work of the authors, Ahlman *et al.* (2009), in which they studied the non-isothermal effects in a turbulent wall-jet.

A schematic of the plane turbulent wall-jet geometry is shown in figure 4.1 where h is the jet inlet height and the x and y axes denote dimensions in the

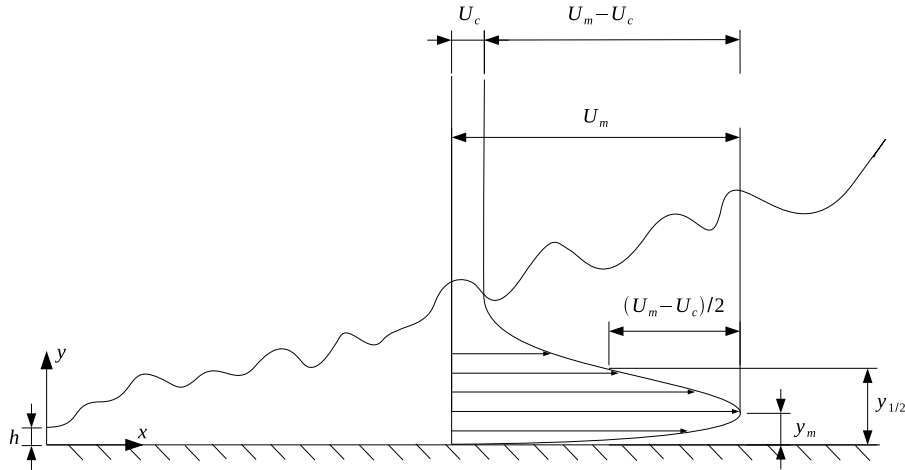


FIGURE 4.1. Schematic of the plane turbulent wall-jet with coflow.

streamwise and wall-normal directions and the spanwise direction is perpendicular to this plane. Here, U_m is the local maximum velocity and U_c is the coflow velocity. For the plane wall-jet with coflow, we define the velocity half-height $y_{1/2}$ as the distance from the wall to the position where the mean velocity is half of the maximum excess value, $U(y_{1/2}) = \frac{1}{2}(U_m - U_c)$.

The structure of a developed turbulent wall-jet can formally be described as two adjacent shear layers of different character. The inner layer, extending from the wall up to the maximum mean streamwise velocity, resembles a thin boundary layer, while the outer part, positioned above the inner layer and reaching out to the ambient flow, can be characterized as a free shear flow. However, there are certain distinctions between the inner layer of wall-jet flows and boundary layer flows. One difference is the intermittent nature of the outer part of the turbulent boundary layer. Another point of difference lies in the modification of the structure of the inner layer of the wall-jet by the turbulence in the outer layer. Furthermore, the skin-friction coefficient of a turbulent boundary layer varies in a different manner from that of the wall-jet. These factors prevent a complete analogy between the inner layer of the wall-jet and the turbulent boundary layer. Considering these restrictions, Hogg *et al.* (1997) concluded that the initial streamwise momentum flux and the kinematic viscosity are suitable parameters governing the flow evolution.

The wall-jet flow seems to be a suitable configuration for examining the interactions between the outer and the inner structures in a turbulent boundary layer. The interaction present in the turbulent plane wall-jet configuration are, in particular, of great interest for the reaction and mixing applications. The turbulent wall-jet is much more flexible and controllable than the boundary

layer. Adding an external coflow to the wall-jet setup will increase the parametric flexibility even further, for instance, by changing the ratio between the free stream velocity and the jet velocity, different flow fields will form. Understanding turbulence structures and the physical dynamics of the problem is however, crucial for analyzing mixing, heat transfer, drag reduction and other phenomena which occur in turbulent wall-jet flows.

4.2. Scalings for compressible turbulent wall-jet

There is a general agreement that the mean velocity profile of the turbulent wall-jet is self-similar, but the scaling parameters are controversial among different researchers. In this section, a very brief introduction to the most commonly used scaling parameters for compressible turbulent plane wall-jet flow is presented. Even though, the present study is not focused on similarities in the inner and outer regions of the wall-jet flow, a rather comprehensive search for the proper scales have been performed and the choice of velocity and length scales for each region is discussed.

If we hypothesize that the inner part of the wall-jet and the inner part of the zero-pressure-gradient boundary layer are similar, it would be appropriate to use the same type of scaling here as well. However, the interaction of large turbulence scales in the outer layer with small scales in the inner layer substantially affects the development of the wall-jet.

4.2.1. Inner layer scaling

The inner-layer scaling for the boundary layer flows was introduced by Prandtl (1932), where appropriate inner length and velocity scales were defined as:

$$l = \frac{\nu}{u_\tau} \quad (4.1)$$

$$u_\tau^2 = \frac{\tau_w}{\rho}, \quad (4.2)$$

where $\tau_w = \rho \nu \left(\frac{\partial U}{\partial y}\right)_{y=0}$ is the wall shear stress and y is the distance from the wall. Performing dimensional analysis in the near-wall region, assuming that the outer effects are negligible, we can acquire universal functions, f and g , for the velocity and Reynolds shear stress as,

$$U^+ = \frac{U}{u_\tau} = f(y^+) \quad (4.3)$$

$$-\overline{uv}^+ = \frac{-\overline{uv}}{u_\tau^2} = g(y^+), \quad (4.4)$$

where $y^+ = y/l$. Relation (4.3) is called *the law of the wall*. A vast number of experimental, analytical, and numerical investigations in wall-bounded flows, including channel flow, pipe flow and boundary layers have been performed to show that the function $f(y^+)$ has a universal form. At the wall, the no-slip condition corresponds to $f(0) = 0$. A Taylor series expansion for small y^+

shows that the linear relation $U^+ = y^+$ is a good approximation in the near-wall region. Simulations and experimental studies of wall-bounded flows show that the linear relation (4.3) is valid for approximately $y^+ < 5$.

4.2.2. Outer layer scaling

Assuming similar characteristics to that of the plane turbulent jet in the outer layer we can define the appropriate outer length and velocity scales as,

$$l_{outer} = y_{1/2} \quad (4.5)$$

$$U_{outer} = U_m. \quad (4.6)$$

The velocity half-height, $y_{1/2}$ was defined as the distance from the wall to the position with a mean velocity of half of the excess value, $U(y_{1/2}) = \frac{1}{2}(U_m - U_c)$. The scalar half-height, $y_{1/2}^\theta$ is the distance to the position where the concentration is half of the maximum concentration, $\Theta(y_{1/2}^\theta) = \frac{1}{2}\Theta_m$.

The friction Reynolds number, Re_τ is defined as

$$Re_\tau = \frac{\delta}{l} = \frac{u_\tau \delta}{\nu_w} = \frac{\delta}{\nu_w^{1/2}} \sqrt{\left(\frac{\partial U}{\partial y}\right)_{y=0}}. \quad (4.7)$$

When an appropriate outer length-scale δ is used, the friction Reynolds number can be seen as an estimate of the outer-layer to inner-layer length-scale ratio. Throughout this study, the half-height of the jet is used as the appropriate outer length scale.

4.2.3. Semi-local scaling

To include a measure for the velocity fluctuations rather than the absolute values of the Favre averaged fluctuation intensities, one approach is to account for the varying mean density by using the semi-local scaling. In this scaling the wall variables are based on the local mean density and viscosity, and their relation to the conventional wall units are

$$u_\tau^* = \sqrt{\frac{\tau_w}{\rho}} = \sqrt{\frac{\rho_w}{\rho}} u_\tau \quad (4.8)$$

$$l^* = \frac{\bar{\nu}}{u_\tau^*} = \frac{\bar{\nu}}{\nu_w} \sqrt{\frac{\rho}{\rho_w}} l, \quad (4.9)$$

The corresponding normalized wall distance becomes

$$y^* = \frac{y}{l^*} \quad (4.10)$$

4.3. DNS of reacting turbulent wall-jets

The numerical code¹ used in the simulations employs a 6th order compact finite difference scheme and a 4th order Runge-Kutta method for spatial and

¹The code has been developed from an original version supplied by Prof. Dr. J. B. Boersma, TU Delft, which is gratefully acknowledged.

TABLE 4.1. Parameters for direct numerical simulations of reacting turbulent wall-jets.

| | Case | Ce | Da | Ze | Re |
|----|---------------------|------|------|------|------|
| I | Isothermal reaction | 0 | 3 | 0 | 2000 |
| II | Exothermic reaction | 38 | 1100 | 8 | 2000 |

temporal integration, respectively, of the fully compressible mass, momentum and energy conservation equations, eqs. (2.1), (2.4) and (??).

The turbulent wall-jet flow contains a broad range of velocity and length scales; and for a simulation to extend to the self-similar region, a large domain is required. The computational domain is a rectangular box, the size of which in terms of inlet jet height, h , is $(L_x = 35h) \times (L_y = 17h) \times (L_z = 7.2h)$ where x , y and z denote the streamwise, wall-normal and spanwise directions, respectively. The number of grid points used in the simulations for both cases presented in table (4.1), are $(N_x = 320) \times (N_y = 192) \times (N_z = 128)$. Several other cases were also computed and are described in paper 2 and paper 3. In the streamwise direction, grid stretching is chosen with a higher resolution in the transition region. At the downstream position $x/h = 25$, where most of the statistics shown in the following sections are taken, the streamwise resolution is about $\Delta x^+ \approx 10$, and the spanwise resolution is about $\Delta z^+ \approx 6$, expressed in wall units. In the wall-normal direction, the grid is finer near the wall to provide sufficient resolution for resolving the inner layer structures. For instance, twelve nodes exist in the near-wall region, below $y^+ = 11$. The Kolmogorov length scale grows with increase in the heat-release, thus, when it comes to the turbulence structures, using similar grids for the two cases means a finer resolution for case II.

The inlet based Reynolds, Mach and Schmidt numbers of the wall-jet are defined by eqs. (2.28), (2.29) and (2.32), respectively. Their numerical values are $Re = 2000$, $M = 0.5$ and $Sc = 0.72$, and the compressibility effects are small as was reported by Ahlman *et al.* (2007). For the heat fluxes, a constant Prandtl number $Pr = \mu c_p / \lambda = 0.72$ is used. The Schmidt number of the scalars is also constant and equal to the Prandtl number.

At the wall, the no-slip condition is fulfilled for the velocity and a no-flux condition, $(\frac{\partial \theta}{\partial y})_{y=0} = 0$, is applied for the scalars. Periodic boundary conditions are used in the spanwise direction. The ambient flow above the jet has a constant coflow velocity of $U_c = 0.10 U_j$ where U_j is the jet inlet velocity. At the top of the domain an inflow velocity of $0.026 U_j$ is used to account for the entrainment. To prevent the reflection and generation of waves, sponge zones are implemented at the inlet and outlet boundaries.

A single-step irreversible reaction as was described in eq. (2.22) is used. In the isothermal reacting wall jet, case I in table (4.1), a simplified reaction term is considered which is a function of density and reactant concentrations and does not depend on temperature, as in eq. (2.25). In the exothermic reacting simulation, case II in table (4.1), an Arrhenius-type reaction rate, according to eq. (2.24), is considered. However, parameters are chosen in a way that the two simulations have comparable rates of fuel consumption throughout the domain. In case I, the reaction is temperature independent and does not release heat. Since the flow is uncoupled from the reaction, the influence of turbulent mixing on the reaction can be studied in the absence of temperature effects. In case II instead, the heat-release effects on turbulence structures can be examined.

The reacting scalars enter the domain separately in a non-premixed manner. At the jet inlet $\theta_{f,j} = 1$, while in the coflow $\theta_{o,c} = 0.5$. Here, $\theta_{f,j}$ is the fuel mass fraction in the fuel stream (the jet flow), and $\theta_{o,c}$ is the oxidizer mass fraction in the oxidizer stream, (the coflow). Thus, using the equations (3.6) for calculating ϕ , the equivalence ratio of the non-premixed flame for the present mixture, we obtain the value $\phi = \frac{\theta_{f,j}}{\theta_{o,c}} = 2$ and using the succeeding relation in chapter 3, eq. (3.8), the value of the stoichiometric mixture fraction is $Z_{st} = 1/3$. Apart from the reactants, a conserved scalar equation is also solved for comparison.

For details of numerical implementations, including the boundary conditions, the grid generation, and also the issues concerning the high wave number disturbances, treatment of occurrences of negative concentrations and the transition to turbulence, see the work by Ahlman (2007). However, the relevant matters for each paper are addressed there accordingly.

4.3.1. *Simulation results*

The following two sections, comprise some important findings of this study. In the first section, some of the key results for the isothermal reacting wall-jet simulations are presented. These findings have a two-fold ground, one is to provide an introduction to the dynamics of a reacting turbulent wall-jet and also to give valuable material for comparison to a following study where heat release is added. In the next section, some of the key statistics and visualizations of the heat-release simulation are presented. However, in the plots shown in this section, the corresponding values of the isothermal case are included for the sake of comparison.

4.3.1.1. *Isothermal reacting turbulent wall-jet*

Visualizations of the instantaneous fields show that the jet is fully turbulent beyond $x/h \approx 15$. Figure 4.2 (a) shows the instantaneous fluctuations of the streamwise velocity in the xz -plane at $y^+ \approx 9$. Elongated streaky structures are clearly observed in the streamwise velocity fluctuation. The velocity fluctuations and the scalar concentration fluctuations have different structures.

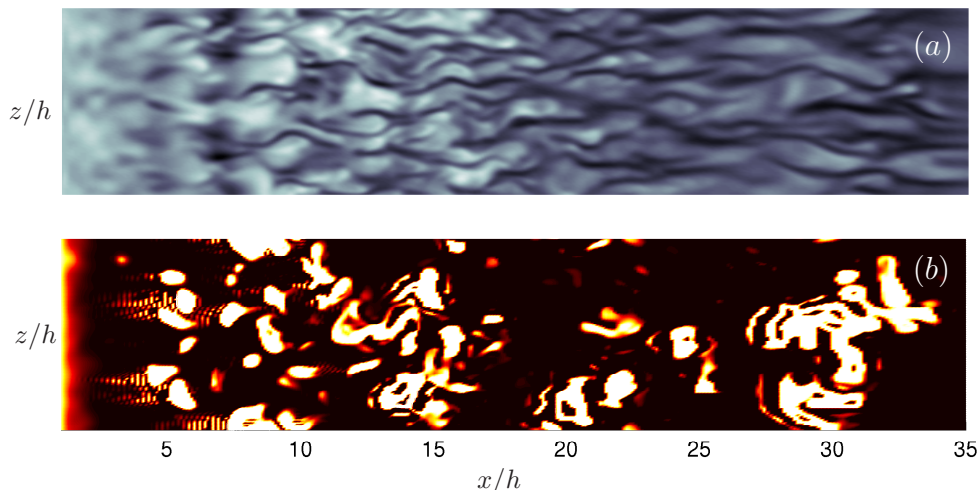


FIGURE 4.2. Instantaneous snapshots of (a) the streamwise velocity fluctuations at a fixed xz -plane; $8 < y^+ < 10$; Light and dark colors represent positive and negative fluctuations, respectively, and (b) the reaction rate at the xz -plane $y/h = 1/2$ ($y^+ = 40$); The lighter color indicates a higher reaction rate.

While the streaky structures of the streamwise velocity fluctuations are apparent, this is not the case for the concentrations and the reaction rate fields. This can be understood from the fact that the mean scalar fields have zero gradient at the wall. The absence of a sharp mean gradient implies that the typical streaky pattern near the wall, seen for the velocity, is not formed for the scalars. Instead, turbulent patches of high concentrations of oxidizer are pumped toward the wall, which result in formation of spots of high reaction rates close to the wall. This is demonstrated in figure 4.2 (b) for the xz -plane at $y^+ = 40$, which is a common behavior in the near-wall region also at lower y^+ values, but the closer to the wall, the fewer are the spots.

As we discussed in chapter 3, the scalar dissipation rate, $\chi = 2\rho\mathcal{D}\overline{\frac{\partial\theta''}{\partial x_i}\frac{\partial\theta''}{\partial x_i}}$, is a quantity which is important in turbulent non-premixed combustion modeling. In non-premixed combustion, reaction takes place when fuel and oxidizer mix on a molecular level and the rate of molecular mixing is expressed by the scalar dissipation rate.

The scalar dissipation rates are shown in figure 4.3 in outer scaling. As for previous statistics, using the outer scaling approximately collapses the scalar dissipation in the outer layer for different downstream positions. From figures 4.3 (a) and 4.3 (b) we note that the dissipation rates of passive and reacting scalars both have rather high values close to the wall, around $y^+ = 10$, where the concentrations are high and the gradients are sharp. However, the

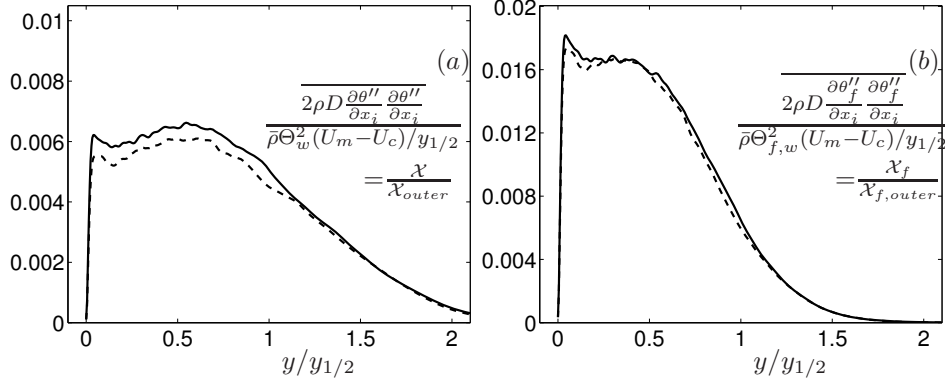


FIGURE 4.3. Passive (a) and reacting (b) scalar dissipations, using outer scaling at different downstream positions; Solid line: $x/h = 21$, dashed line: $x/h = 25$.

normalized fuel dissipation rate is almost two times larger than that of the passive scalar, indicating larger gradients for fuel species, while it is smaller in the outer part of the jet. There is a wide flat region in the passive scalar dissipation profile, $0.1 < y/y_{1/2} < 1$ which evidently is shorter in the fuel dissipation profile $0.1 < y/y_{1/2} < 0.5$, which indicates that the passive scalar has a more homogeneous small-scale mixing throughout the jet. Beyond this position, a sudden decrease begins in both of the dissipation profiles. The reaction has two competing effects on the scalar dissipation value, one is to sharpen the scalar gradients resulting in high dissipation rates, and the other is to consume the reacting scalar, leading to lower dissipation rates. Beyond the half-height of the jet, i.e. $y/y_{1/2} = 1$, much of the fuel has been consumed. Due to the lower concentration of the fuel, the dissipation rate decreases and has smaller values than that of the conserved scalar.

The probability density functions (PDFs) of reacting species as well as the passive scalar are examined at different downstream positions to shed light on the mixing characteristics of the flow. At each downstream position, several wall-normal planes are considered. The height of each plane is normalized with the local half-height of the jet. In the fully turbulent region, the PDFs of the species are rather similar, therefore, only one downstream position is shown here, i.e. $x/h = 25$, see figure 4.4. The PDFs of the fuel and the passive scalar are rather similar from the wall up to the vicinity of the half-height of the jet, $y/y_{1/2} = 1$ plane, but beyond this position the passive scalar PDF still keeps its near-Gaussian shape while the fuel PDF has a large peak at low concentrations showing that much of the fuel has been consumed. The PDFs of the fuel concentration have long exponential tails in the outer shear layer, which is an evidence for the existence of high intermittency. Worth to notice is that the shape of the fuel and oxidizer PDF curves are most similar at the

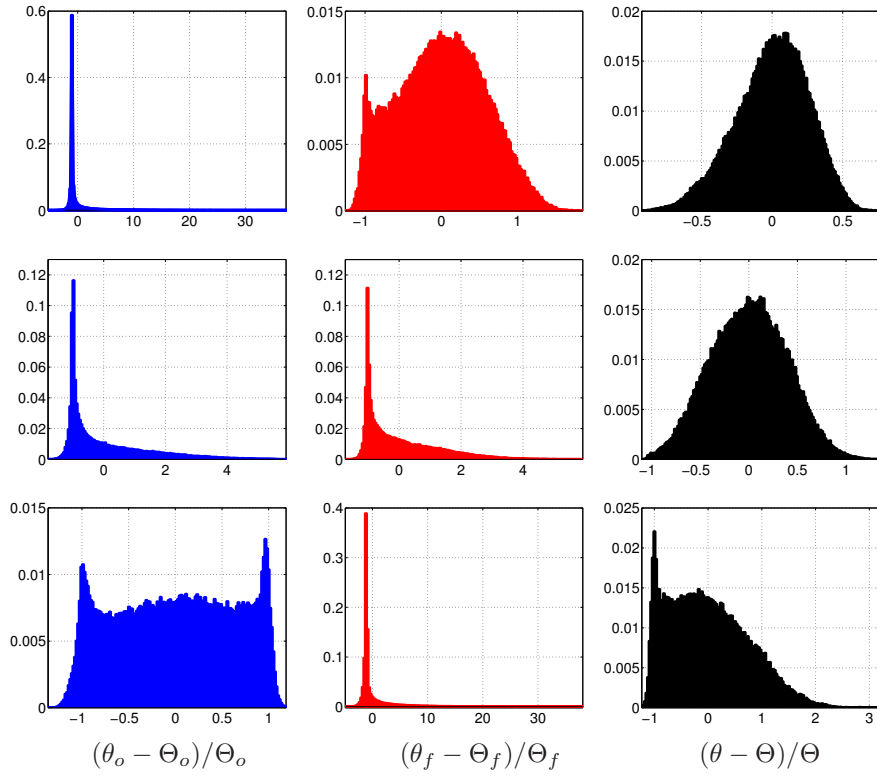


FIGURE 4.4. Probability density functions of different species at $x/h = 25$ at several wall-normal locations are shown in rows, top: $y/y_{1/2} = 0.5$, middle: $y/y_{1/2} = 1$ and bottom: $y/y_{1/2} = 1.5$. Minimum and maximum concentrations in each plot match the borders of plot and zero on x-axis points to the mean concentration.

half-height planes at any downstream position. The oxidizer PDFs are close to the minimum concentration values close to the wall which is a reasonable behavior considering the oxidizer concentration profile. Moving away from the wall, the PDF profile becomes broader and around $y/y_{1/2} = 1.5$ another peak occurs in the PDF of the oxidizer which is close to the maximum concentration. This implies that the probability of particles with low concentrations coming from the wall region or caused by reaction with the fuel and particles with high concentrations coming from outer region are both high at this position. Hence, the formation of these two peaks. The peak at the minimum concentration disappears around $y/y_{1/2} = 2$.

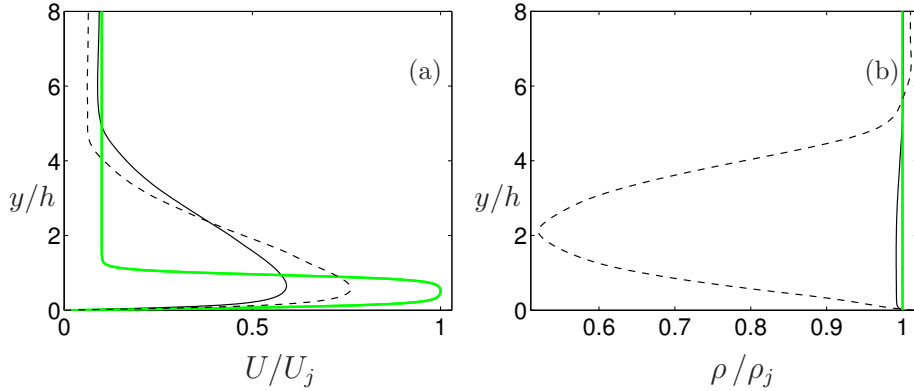


FIGURE 4.5. Mean cross-stream profiles of (a) streamwise velocity and (b) density at $x/h = 25$; Solid line: case I, dashed line: case II. The respective profiles at inlet are shown in thick solid green.

4.3.1.2. Exothermic reacting turbulent wall-jet

To provide an overview of the turbulence structures and the temperature rise of the flow field in the exothermic turbulent wall-jet simulation, the instantaneous snapshots of the streamwise velocity and the temperature fields are visualized in figure 1.2. The flow is from left to right and is evolving in space. The streamwise velocity is scaled with the jet inlet velocity and the temperatures are given in Kelvin. The reaction starts immediately after the inlet and is spreading as the flow evolves in the downstream direction. A significant amount of heat is released as it can be observed in figure 1.2. High temperatures influence the development and dynamics of the wall-jet through density changes, which are caused by gas expansion.

Cross-stream profiles of the mean streamwise velocity and density are shown in figure 4.5. The density changes, figure 4.5 (b), in the chemically reacting case are significant and the average density may reach values as low as almost half of the inlet value. The streamwise velocity, figure 4.5 (a), illustrates the resulting acceleration of the flow for case II, which has the highest temperature. The increase in the maximum excess value, i.e. $(U_m - U_c)$, is about 40% for this case at $x/h = 25$.

The skin friction coefficient is an important quantity and the information about its characteristics are crucial for calculation of the mass and convective heat transfer. However, the accurate experimental determination of the skin friction still remains to be a major challenge in turbulent wall-jet flows.

The skin friction drag can in some combustion applications be important for the overall performance of the combustor. Numerous techniques exist for the reduction of viscous losses in different applications. The boundary layer

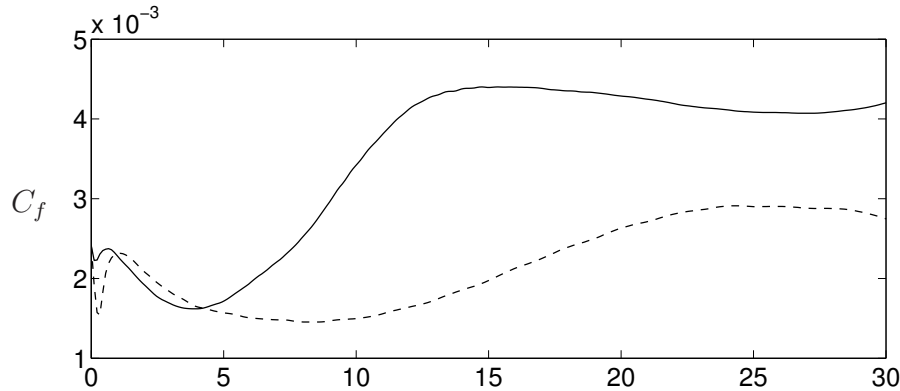


FIGURE 4.6. Downstream development of the skin friction coefficient; Solid line: case I, dashed line: case II.

combustion represents a method of reducing drag mainly in hypersonic applications. Recent experimental results show that boundary layer combustion can be used to reduce turbulent skin friction drag and hence increase the net thrust output, see e.g. Chan *et al.* (2010). The combustion in the near-wall region, releases heat and increases the temperature in the boundary layer which reduces the density and Reynolds stresses, that results in a reduction of the turbulent skin friction drag.

In the turbulent wall-jet configuration, the skin friction coefficient is slightly higher than the corresponding boundary layer flow. However, in the real working condition, the typical surface roughness is believed to increase the skin friction up to 30% at moderate Reynolds numbers, (Tachie *et al.* 2004). Therefore, the near-wall combustion may be used not only to compensate that, but even to further decrease the overall drag coefficient.

In the present case the flow is subsonic, but it may still be of interest to evaluate the effect of combustion on the skin friction coefficient. The values of the skin friction coefficients, $C_f = 2(\frac{u_\tau}{U_m})^2$ are shown in figure 4.6 for cases I and II. At the downstream position $x/h = 15$, for instance, in the transition region, the C_f coefficient has been reduced more than 55% which mainly can be attributed to the delayed transition. In the fully turbulent region, at $x/h = 25$, this reduction is about 30%. These reductions in the skin friction coefficient are similar to those reported in the experimental studies by Suraweera *et al.* (2005) and Chan *et al.* (2010).

The scalar dissipation rate is a quantity of prominent importance in non-premixed combustion, and we have shown how the scalar dissipation rate behaves in the isothermal reacting wall-jet simulation, see figure 4.3. The heat-release effects on scalar dissipation rates are illustrated in figure 4.7 where the iso-contours of the scalar dissipation rate for case I and case II are shown. The fields are plotted on a logarithmic scale to accentuate their wide dynamic range.

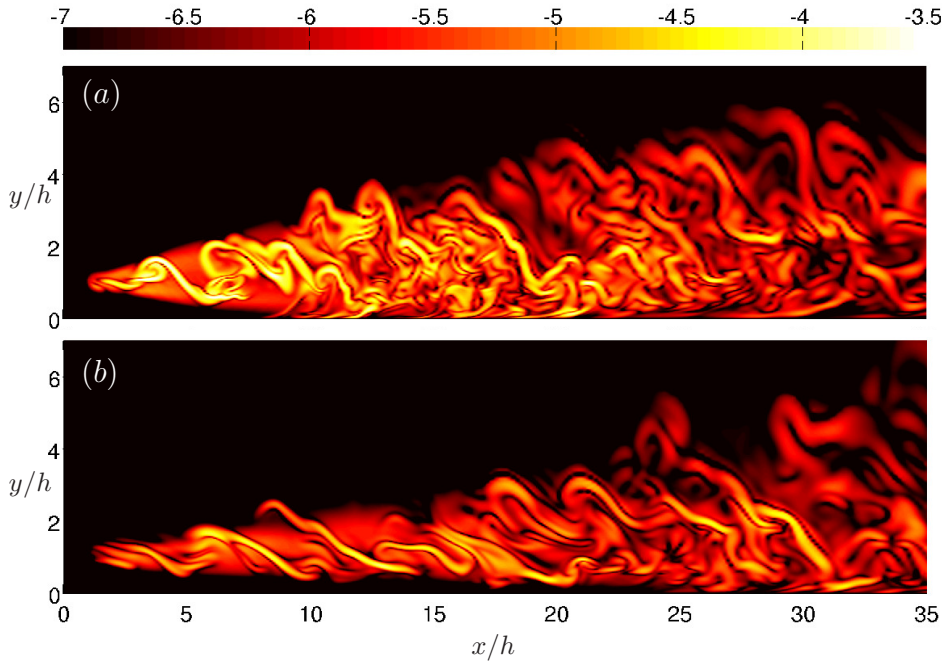


FIGURE 4.7. Iso-contours of the logarithm of the scalar dissipation rate, $\log_{10}(\chi)$, for (a) case I and (b) case II.

The flow is fully turbulent in both cases and long thin sheet-like structures are observed, similar to what is reported by Hawkes *et al.* (2007). These figures show less fine-scale structures in the dissipation rate field of case II, indicating damping of small scales due to heat-release effects.

Heat-release effects modify the flow field and the wall-jet dynamics in several ways. One is the effect on the turbulence structures, which in turn influences mixing. Heat release influences on turbulence scales can be illustrated by examining the two-dimensional spectra. Studying the two-dimensional spectra, $E_{uu}^{z*} = \lambda_z \Phi_{uu} / u_\tau^{*2}$, gives a more comprehensive insight into the scale variation throughout the wall-normal axis, see del Álamo & Jiménez (2003).

The premultiplied two-dimensional spectra of the streamwise velocity fluctuations in the spanwise direction are shown in figure 4.8 in inner units. Here, we have used the semi-local inner scaling, as explained in eq. (4.8), $E_{uu}^{z*} = \lambda_z \Phi_{uu} / u_\tau^{*2}$. A corresponding wavelength in the semi-local scaling as $\lambda_z^* = \frac{2\pi}{\kappa_z} u_\tau^* / \nu$, could not be defined, since due to the density variation along the wall-normal axis, a different wavenumber for each wall-normal location and therefore different wavelengths would be needed. Thus, the local half-height of each jet has been used to demonstrate the corresponding wavelengths. The figure confirms that the inner peak location is located approximately at the

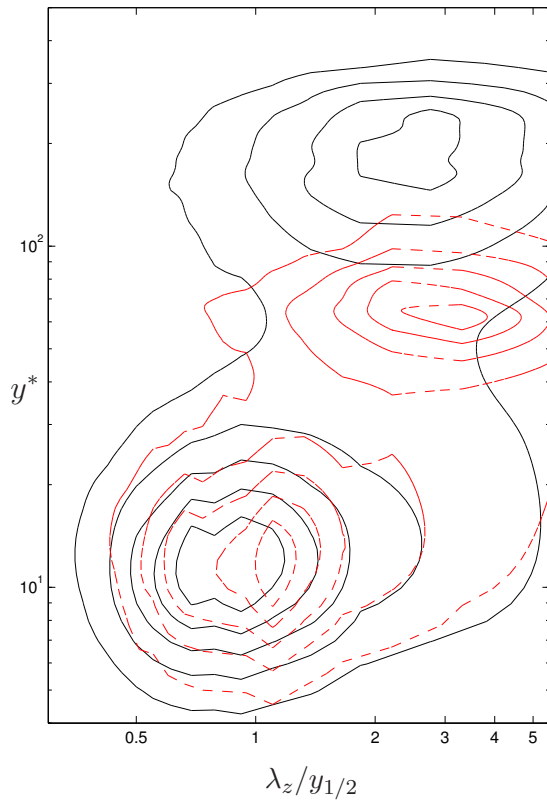


FIGURE 4.8. Premultiplied spanwise spectra, $E_{uu}^{z*} = \lambda_z \Phi_{uu} / u_\tau^{*2}$, of the streamwise velocity fluctuations, case I (black, solid) and case II (red, dashed), scaled in the semi-inner scaling; Downstream position $x/h = 25$.

same distance from the wall for both cases I and II, but for the heat release case the peak is shifted to somewhat larger scales. The location of the outer peak is shifted significantly toward the inner region due to the heat release effects, and to slightly larger scales.

CHAPTER 5

Summary of the papers

Paper 1

Direct numerical simulation of an isothermal reacting turbulent wall-jet

We have performed direct numerical simulation (DNS) of a reacting turbulent wall-jet. A single-step global reaction is considered in which the reaction rate is temperature independent. In this study, we have neglected thermal effects of the chemical reaction intentionally, in order to exclusively concentrate on the turbulent flow effects on the isothermal reaction. Fuel and oxidizer enter the computational domain in two separate streams, the jet flow consist of fuel and the coflow contains the oxidizer species.

The turbulent statistics of the present DNS are validated against previous DNS of a non-reacting turbulent wall-jet. To shed light on turbulent mixing effects on concentration fields in near-wall regions, a detailed study of the probability density functions (PDF) is carried out. The comparison between the reacting scalars PDF and the passive scalar PDF throughout the domain, reveals the significance of the reaction influence and the wall effects on the scalar distributions. A detailed discussion about the scalar dissipation rate of conserved and reacting scalars is included. Further, we have examined the higher order moments of the scalar concentrations as well as the velocities. The higher order moments for velocities exhibit a similar behavior to those of other wall-bounded flows. Moreover, a comparison between the third order moments of velocities with recent experimental measurements is made, which shows an acceptable correspondence. Interesting differences in the higher order statistics of passive and reacting species concentrations are detected in near-wall regions. Furthermore, we have exposed the fundamental features of the reaction rate and the stoichiometric mixture surface in the isothermal reacting turbulent wall-jet.

Paper 2

Heat release effects on mixing scales of turbulent reacting wall-jets, a direct numerical simulation study

This study concerns the role of heat release in chemically reacting turbulent

wall-jet flows, where DNS of several chemically reacting turbulent wall-jets including significant amounts of heat release is performed. The main aim of this investigation is to examine the heat-release effects on different scales of turbulence. The "turbulence-chemistry" or more precisely "turbulence-heat release" interactions are illustrated by studying the modifications of different large and mixing scales. The influence of heat release on different turbulence and reactants statistics is investigated.

Primarily, it is observed that heat release effects delay the transition process in the chemically reacting cases and enlarge the fluctuation intensities of density and pressure. Heat release also enhances the fluctuations level of the species concentrations. However, it has a damping effect on all velocity fluctuation intensities as well as the Reynolds shear stress. The turbulent kinetic energy behavior in different cases is examined, using different scalings. Mixing scales are visualized by exploring the dissipation rate of the fuel and passive scalar concentrations. We observed much finer structures in isothermal reacting turbulent wall-jet and found that heat release modifies both the instantaneous field characteristics and the mean values of the scalar dissipation rates. With aid of vortex diagnosing tools, the stoichiometric mixture fraction surface and the two-point correlations of velocities, we have identified heat-release consequences on different scales. Larger vortices are detected in simulations with higher amount of heat-release.

Further analysis using one-dimensional and two-dimensional premultiplied spectra of the streamwise velocity are performed, where the results indicate a shifting in the position of the outer peak of the energy spectra. Moreover, probability density functions of reactants are shown to be affected by heat release effects. Finally, the scatter plots of temperature fields against the mixture fraction are also studied at different locations.

Paper 3

Numerical investigation of wall heat transfer and skin-friction coefficient in reacting turbulent wall-jets

This study is focused on wall heat transfer and is an extension of the study described in paper 2. The main aim of this study is to examine the statistics of the turbulent wall-jet which are particularly important in wall heat transfer applications. The wall heat flux increases in chemically reacting cases due to the substantial temperature rise in the flow field, but, the corresponding Nusselt number decreases with the increase of heat release. Further, the near-wall reaction effects on the skin friction coefficient are addressed, where it is shown that the skin friction coefficient is considerably reduced due to the near-wall reaction. The near-wall reaction characteristics are further examined through the instantaneous snapshots of the reaction rate for different cases.

Outlook

As the future plan of this work, DNS can be used to study the flame-wall interaction in more detail. As a single-step global chemistry approach does not include information about radical formation and recombination, it cannot fully predict all the near wall characteristics of turbulent chemistry interaction. Therefore, the objective is to introduce a multi-step reaction, which includes sufficient chemistry that enables us to extract detailed information about the flame-wall interaction. This reduced chemistry should not necessarily stand somewhere high up in the hierarchy of the reduced chemistry models, as our purpose may even be achieved by the four-step mechanism of methane-air reaction. Considering the spatial and temporal resolutions needed for the computations, the chemistry models may be reconsidered and might change to simpler or more advanced approaches.

Apart from chemistry, the flow configuration and the boundary conditions in different simulations are kept similar. Another appropriate next step for this project can be the implementation of different wall boundary conditions. So far, we have considered an isothermal wall, which can be altered to, for instance, an adiabatic wall. Furthermore, the effects of preheating of the oxidizer stream can be studied by increasing the coflow temperature or even by adding a second warmer pilot-flow close to the jet nozzle.

Another possibility would be to perform simulations at a higher Reynolds number, to seek information about the possible differences of the mixing scenario in the near-wall region and the impact on the flame structure from the increased scale separation between the inner and outer regions.

Moreover, the DNS results presented in this work can be used for evaluation of non-premixed combustion models and also for development and validation of compressible turbulent subgrid-scale models.

Acknowledgments

I would like to acknowledge my supervisor Prof. Arne V. Johansson for his supportive accompaniment, his overwhelming guidance, enthusiastic leadership and encouraging inspirations throughout this work. Thanks a lot Arne, for generously sharing your vast knowledge of fluid mechanics and turbulence in particular with me.

I would like to acknowledge my co-advisor Dr. Geert Brethouwer and also Dr. Setfan Wallin and Amin Rasam for their different helps, useful discussions and valuable inputs to this work.

This project has been financed by the Swedish Centre for Combustion Science and Technology (CECOST), which I would like to gratefully acknowledge that and also specially thank all members of "modeling and validation group". I would like also to thank the Swedish National Infrastructure for Computing (SNIC) for providing the computer time and convey my deepest gratitude to the support team at PDC.

This thesis has been read by Prof. Laszlo Fuchs, Dr. Ramis Örlü and Amin Rasam, their feedback and useful comments are very much appreciated.

I would like to thank my officemates for the pleasant working atmosphere in our room and many thanks to colleagues at Mechanics department of KTH; You make it a pleasure for me to come to work everyday, I would like to specially name, Natalia Kosterina, Ruoli Wang, Dr. Tobias Strömgren, Dr. Ardeshir Hanifi, Carolina Eneqvist, Seif Dalilsafaei, Johan Malm, Enrico Deusebio, Robert Pettersson, Onofrio Semeraro, Armin Hosseini, Florian von Stillfried, Marit Berger, Dr. Antonios Monokrousos, Iman Lashgari, David Tempelmann, Solmaz Akbaripur, Qiang Li, Lailai Zhu, Dr. Ruth Lambert, Dr. Eva Voronkova, Dr. Lars-Uve Schrader, Dr. Daniel Ahlman, Reza Dadfar, Dr. Outi Tammissola, Shahab Shahinfar, Ylva Odemark, Sohrab Sattarzadeh, Peter Lenaers, Werner Lazeroms, Azad Noorani, Steven van Wyk, Olesya Klets, Krishnagoud Manda, Andreas Carlson, Sasan Sarmast, Dr. Andreas Vallgren, Yue Wang, Joy Klinkenberg and Amer Malik.

Finally, I would like to thank my parents, my sisters and brother and all other family members, for their constant care, support and encouragements, and my very special thanks to my wonderful husband, for his understanding, unconditional love and endless support.

Bibliography

- AHLMAN, D. 2007 Numerical studies of turbulent wall-jets for mixing and combustion applications. PhD thesis, Royal Institute of Technology, KTH, Stockholm, Sweden.
- AHLMAN, D., BRETTHOUWER, G. & JOHANSSON, A. V. 2007 Direct numerical simulation of a plane turbulent wall-jet including scalar mixing. *Phys. Fluids* **19**, 065102.
- AHLMAN, D., VELTER, G., BRETTHOUWER, G. & JOHANSSON, A. V. 2009 Direct numerical simulation of non-isothermal turbulent wall-jets. *Phys. Fluids* **21**, 035101.
- BILGER, R. W. 2000 Future progress in turbulent combustion research. *Prog. Energy Combust. Sci.* **26**, 367–380.
- BRADSHAW, P. & GEE, M. T. 1960 Turbulent wall-jets with and without external stream. *Aeronautics Research Council Reports and Memoranda No. 3252*.
- BRUNEAUX, G., AKSELVOLL, K., POINSOT, T. & FERZIGER, J. H. 1996 Flame-wall interaction simulation in a turbulent channel flow. *Combust. Flame* **107**, 27–44.
- BRUNEAUX, G., POINSOT, T. & FERZIGER, J. H. 1997 Premixed flame-wall interaction in a turbulent channel flow: budget for the flame surface density evolution equation and modeling. *J. Fluid Mech.* **349**, 191–219.
- CHAN, W. Y. K., MEE, D. J., SMART, M. K., TURNER, J. C. & STALKER, R. J. 2010 Boundary layer combustion for viscous drag reduction in practical scramjet configurations. *27th International Congress of The Aeronautical Sciences, Nice, France*. pp. 1–10.
- CHEN, J. H. 2011 Petascale direct numerical simulation of turbulent combustion—fundamental insights towards predictive models. *Proc. Combust. Inst.* **33**, 99–123.
- CONAIRE, M. O., CURRAN, H. J., SIMMIE, J. M., PITZ, W. J. & WESTBROOK, C. K. 2004 A comprehensive modeling study of hydrogen oxidation. *Int. J. Chem. Kinet.* **36**, 603–622.
- CONLON, B. P. & LICHTER, S. 1995 Dipole formation in the transient planar wall-jet. *Phys. Fluids* **7**, 99–114.
- DABRIEU, F., CUENOT, B., VERMOREL, O. & POINSOT, T. 2003 Interaction of flames of $H_2 + O_2$ with inert walls. *Combust. Flame* **135**, 123–133.
- DEJOAN, A. & LESCHZINER, M. A. 2005 Large eddy simulation of a plane turbulent wall jet. *Phys. Fluids* **17**, 025102.

- DEL ÁLAMO, J. C. & JIMÉNEZ, J. 2003 Spectra of the very large anisotropic scales in turbulent channels. *Phys. Fluids* **15** (6), 41–44.
- DEY, S., NATH, T. K. & BOSE, S. K. 2010 Submerged wall-jets subjected to injection and suction from the wall. *J. Fluid Mech.* **653**, 57–97.
- DOPAZO, C. 1994 Recent developments in pdf methods. *Turbulent Reacting Flows, Academic Press London*, pp. 375–476.
- ERIKSSON, J. G., KARLSSON, R. I. & PERSSON, J. 1998 An experimental study of a two-dimensional plane turbulent wall jet. *Exp. Fluids* **25**, 50–60.
- FÖRTHMANN, E. 1934 Über turbulente Strahlausbreitung. *Ing. Arch.* **5**, 42–54.
- FUREBY, C. 2008 Towards the use of large eddy simulation in engineering. *Prog. Aerosp. Sci.* **44**, 381–396.
- GEORGE, W. K., ABRAHAMSSON, H., ERIKSSON, J., KARLSSON, R. I., LÖFDAHL, L. & WOSNIK, M. 2000 A similarity theory for the turbulent plane wall jet without external stream. *J. Fluid Mech.* **425**, 367–411.
- GLAUERT, M. B. 1956 The wall jet. *J. Fluid Mech.* **1**, 625–643.
- GOGINENI, S., VISBAL, M. & SHIH, C. 1999 Phase-resolved PIV measurements in a transitional plane wall jet: a numerical comparison. *Exp. Fluids.* **27**, 126.
- GRUBER, A., SANKARAN, R., HAWKES, E. R. & CHEN, J. H. 2010 Turbulent flame-wall interaction: a direct numerical simulation study. *J. Fluid Mech.* **658**, 5–32.
- HALL, J. W. & EWING, D. 2010 Spectral linear stochastic estimation of the turbulent velocity in a square three-dimensional wall jet. *J. Fluids Eng.* **132** (051203).
- HAWKES, E. R., SANKARAN, R., SUTHERLAND, C. & CHEN, J. H. 2007 Scalar mixing in direct numerical simulations of temporally evolving plane jet flames with skeletal CO/H₂ kinetics. *Proc. Combust. Inst.* **31**, 1633–1640.
- HILBERT, R., TAP, F., EL-RABII, H. & THÉVNIN, D. 2004 Impact of detailed chemistry and transport models on turbulent combustion. *Prog. Energy Combust. Sci.* **30**, 61–117.
- HOGG, A. J., HUPPERT, H. E. & DADE, W. B. 1997 Erosion by planar turbulent wall jets. *J. Fluid Mech.* **338**, 317–340.
- HUNT, J. C., WRAY, A. A. & MOIN, P. 1988 Eddies, stream and convergence zones in turbulent flows. *Tech. Rep. CTR-S88, Center for turbulence research, Stanford University*.
- KNAUS, R. & PANTANO, C. 2009 On the effect of heat release in turbulence spectra of non-premixed reacting shear layers. *J. Fluid Mech.* **626**, 67–109.
- LAUNDER, B. E. & RODI, W. 1981 The turbulent wall jet. *Prog. Aerospace. Sci* **19**, 81–128.
- LEVIN, O., CHERNORAY, V. G., LÖFDAHL, L. & HENNINGSON, D. S. 2005 A study of the Blasius wall jet. *J. Fluid Mech.* **539**, 313–347.
- NARASHIMA, R., NARAYAN, K. Y. & PARTHASARATHY, S. P. 1973 Parametric analysis of turbulent wall jets in still air. *Aeronaut. J.* **77**, 335.
- NEUENDORF, R. & WYGNANSKI, I. 1999 On a turbulent wall jet flowing over a circular cylinder. *J. Fluid Mech.* **381**, 1–25.
- O'BRIEN, E. E. 1980 The probability density function (pdf) approach to reacting turbulent flows. *Turbulent Reacting Flows, Academic Press London* p. 185.
- PETERS, N. 2000 Turbulent combustion. Cambridge University Press.
- POINSOT, T., CANDEL, S. & TROUVÉ, A. 1996 Applications of direct numerical

- simulation to premixed turbulent flames. *Prog. Energy Combust. Sci.* **21**, 531–576.
- POINSOT, T., HAWORTH, D. C. & BRUNEAUX, G. 1993 Direct simulation and modeling of flame-wall interaction for premixed turbulent combustion. *Combust. Flame* **95**, 118–132.
- POINSOT, T. & VEYNANTE, D. 2001 *Theoretical and Numerical Combustion*. R.T. Edwards.
- POPE, S. B. 1985 Pdf method for turbulent reacting flows. *Prog. Energy Combust. Sci.* **11**, 119–195.
- PRANDTL, L. 1932 Zur turbulenten Strömung in Rohren und längs Platten. *Ergebn. Aerodyn. Versuchsanst. Göttingen* **4**, 18–29.
- RILEY, J. J. 1998 Turbulent combustion modelling. In *Transition, Turbulence and Combustion Modelling, Ercoftac Series* (ed. A. Hanifi, H. Alfredsson, A. V. Johansson & D. Henningson). Kluwer academic publishers.
- RUETSCH, G. R., VERVISCH, L. & LINAN, A. 1995 Effects of heat release on triple flames. *Phys. Fluids* **7**, 1447–1454.
- SURAWEERA, M., MEE, D., & STALKER, R. 2005 Skin friction reduction in hypersonic turbulent flow by boundary layer combustion. *43rd AIAA Aerospace Sciences Meeting and Exhibit, Reno, Nevada* .
- TACHIE, M. F., BALACHANDAR, R. & BERGSTROM, D. J. 2004 Roughness effects on turbulent plane wall jets in an open channel. *Experiments in Fluids* **37**, 281–292.
- URNS, S. R. 1993 *An introduction to combustion*. McGraw Hill.
- VERVISCH, L. 2000 Using numerics to help the understanding of non-premixed turbulent flames. *Proc. Combust. Inst.* **28**, 11–24.
- VERVISCH, L. & POINSOT, T. 1998 Direct numerical simulation of non-premixed turbulent flames. *Annu. Rev. Fluid Mech.* **30**, 655–691.
- VERVISCH, L. & VEYNANTE, D. 2011 Turbulent Combustion. Von Karman Institute for Fluid Dynamics.
- VEYNANTE, D. & VERVISCH, L. 2002 Turbulent combustion modeling. *Prog. Energy Combust. Sci.* **28**, 1–138.
- VISBAL, M., GAITONDE, D. V. & GOGINENI, P. 1998 Direct numerical simulation of forced transitional plane wall jet. *AIAA paper, 98-2643* .
- WANG, Y. & TROUVÉ, A. 2006 Direct numerical simulation of nonpremixed flame-wall interactions. *Combust. Flame* **144**, 461–475.
- WERNZ, S. & FASEL, H. F. 1996 Numerical investigation of unsteady phenomena in wall jets. *AIAA paper, 96-0079* .
- WERNZ, S. & FASEL, H. F. 1997 Numerical investigation of forced transitional wall jets. *AIAA paper, 97-2022* .
- WESTBROOK, C. K., MIZOBUCHI, Y., POINSOT, T. J., SMITH, P. J. & WARNATZ, J. 2005 Computational combustion. *Proc. Combust. Inst.* **30**, 125–157.
- WILLIAMS, F. A. 1985 *Combustion Theory*, 2nd edn. Benjamin/Cummings.
- WYGNANSKI, I., KATZ, Y. & HOREV, E. 1992 On the applicability of various scaling laws to the turbulent wall jet. *J. Fluid Mech.* **234**, 669–690.
- ZHOU, M. D., HEINE, C. & WYGNANSKI, I. 1996 The effects of excitation on the coherent and random motion in a plane wall jet. *J. Fluid Mech.* **310**, 1–37.